

CFD study of nasal drug delivery

Inés Herrero Turégano

Master thesis submitted under the supervision of
Prof. Benoit Haut

The co-supervision of
Prof. Pierre Lambert

Academic year
2018-2019

In order to be awarded the Master's Degree in
MSc in Chemical and Materials Engineering

ABSTRACT

Title: CFD study of nasal drug delivery

Author: Inés Herrero Turégano

Master's degree in Chemical and Materials Engineering

Academic year: 2018 – 2019

In the last decades, the increasing number of neurodegenerative diseases have alerted the scientific community. The diagnosis of Alzheimer disease is supposed to double the number every 20 years, reaching the 131,5 million by 2050. Some studies have shown a relation between the loss of smell and the appearance of these kinds of neurodegenerative diseases. For this reason, the nasal cavity is considered a potential pathway to treat the disease since the olfactory epithelium offers a direct connection to the brain. In addition, nasal delivery overcomes some of the limitations that oral and parental techniques involve such as a slower delivery process to the brain, low concentration of the drug in the brain due to the existence of a blood brain barrier or a low bioavailability of the drug in the brain.

In this context, the aim of this thesis is to study the air flow behaviour of human breathing in the nasal cavity by using a computational fluid dynamics (CFD) simulating software, ANSYS Fluent. The aim of these simulations is to obtain an accurate description of the airflow behaviour in order to know which areas of the nasal cavity are more exposed to the drug effects. Different real situations are simulated: normal human breathing, strong conditions of human breathing like the action of sniffing drugs and lastly the particle's injection.

From this study, future research can be developed to maximize the nasal drugs delivery in some locations by varying the formulation of the drug or the administration technique.

Keywords: CFD, modelling, nasal drug delivery, flow behaviour

ACKNOWLEDGEMENTS

I would like to acknowledge everyone who played a role in my academic accomplishments. First of all, my family, who have always supported me in my studies. Secondly, personal in TIPS department who has figure out many of my doubts during the elaboration of this thesis, especially professor Benoit Haut, who has led me in the steps to follow for the elaboration of this thesis. Thirdly, some of my pharmaceutical friends, who have provided me some valuable data for the simulations of this project and have shared its knowledge about the pharmaceutic field, specially mention to Maria Dolores and Amparo. Last but not least, my dear friends who have lived with me during this enriching stayment abroad in Brussels. You have been like my family.

TABLE OF CONTENTS

ABSTRACT	3
ACKNOWLEDGEMENTS	5
1. OBJECTIVE	10
2. INTRODUCTION	11
2.1. Neurodegenerative diseases.....	11
2.1 Nasal Anatomy	13
2.2 Intranasal drug delivery	14
2.3 Constraints on the nasal drug delivery.	15
3. MATHEMATICAL MODEL (EQUATIONS AND BOUNDARY CONDITIONS).	16
Development of generic Flow Models	16
Conservation of Mass.....	16
Consevation of Momentum	17
Mapping these Models onto CFD Solver.....	17
Finite Volume (FV) method.	17
4. SET-UP THE MODEL IN ANSYS	18
4.1. Import and edit the STL file.....	18
4.2. Meshing.....	18
4.3. Set-Up.....	21
4.3.1. Set-up domain	21
4.3.2. Set-up Physics.....	21
4.3.3. Models.....	21
4.3.4. Materials.	23
4.3.5. Zones	23
4.4. Solution	25
4.5. Post-processing results	26
4.5.1. Contour plane.....	26
4.5.2. Volume Rendering.....	26
4.5.3. Streamline	27
5. MESH INDEPENDENCE STUDY.	28
6. MODELS.....	37
Model 1. Normal conditions breathing imposing the mass flow air.....	37
Model 2. Normal conditions breathing imposing pressure outlet.....	37
Model 3. Sniffing. Extreme conditions breathing.	37
Model 4. Particle's injection.....	38

7. POST-PROCESSING RESULTS.....	39
Model 1. Normal conditions breathing imposing the mass flow air.....	39
Model 2. Normal conditions breathing imposing pressure outlet.....	41
Model 3. Sniffing. Extreme conditions breathing.	45
Comparison of the results 3 with model 1:.....	48
Model 4. Particle's injection.....	49
8. CONCLUSIONS	51
REFERENCES	52
APPENDICES	53
ANSYS FLUENT.....	53
1.1. Quality of the mesh.....	53
1.1.1. Aspect ratio	54
1.1.2. Resolution of the mesh	56
1.1.3. Skewness	56
1.1.4. Smoothness.....	56
1.1.5. Flow-Field Dependency.....	56
1.1.6. Monitoring Residuals	57

Figure 1. Olfactory mechanism and the related anatomy, with a global view of the nasal cavity on the right and a detailed view of the tissues that cover the roof of the olfactory cleft on the left.	11
Figure 2. Number of people with dementia in low and middle income countries compared to high income countries.....	12
Figure 3. Anatomy of the human nasal cavity (NALT: Nasopharynx-associated lymphatic tissue)	13
Figure 4. Mechanisms of drug transport from the nasal cavity to the brain	14
Figure 5. Display of the nose.	18
Figure 6. Nodes and elements of first mesh.	19
Figure 7. Details of the first mesh with a cell size of 0,5 mm.	20
Figure 8. Details of the selected Patch Conforming Method.....	20
Figure 9. Set units.....	21
Figure 10. Setting up physics parameters.	21
Figure 11. Selected model in set up physics.	22
Figure 12. Create materials.	23
Figure 13. Cell zone conditions set up.....	24
Figure 14. Boundary conditions inlet set up	24
Figure 15. Boundary conditions outlet set up.....	25
Figure 16. Solution Method set up.....	25
Figure 17. Residuals for cell size of 0,5 mm.	26
Figure 18. Velocity contour left nostril	26
Figure 19. Velocity contour right nostril	26
Figure 20. Volume rendering of the airflow velocity	27
Figure 21. Streamline tool.....	27
Figure 22. Scaled residuals plot of the first mesh	29
Figure 23. Pressure outlet of the first mesh.....	29
Figure 24. Scaled plot residuals of the second mesh.....	30
Figure 25. Scaled residuals plot of the third mesh.....	30
Figure 26. Pressure Outlet of the second mesh.....	31
Figure 27. Scaled residuals plot of the fourth mesh	31
Figure 28. Pressure Outlet of the fourth mesh	32
Figure 29. Scaled residuals plot of the fifth mesh.....	32
Figure 30. Pressure Outlet contour fifth mesh	33
Figure 31. Scaled residuals plot of cell size 0,7 mm	33
Figure 32. Pressure Outlet contour sixth mesh.....	34
Figure 33. Residuals of cell size of 0,37 mm.....	34
Figure 34. Pressure Outlet contour seventh mesh	35
Figure 37. Residuals plot model 1.	39
Figure 38. Contour Pressure on Right Nostril	Figure 39. Contour pressure on Left Nostril.....
Figure 40. Residuals plot model 2	41
Figure 41. Pressure volume rendering model 2	41
Figure 42. Velocity Volume Rendering Model 2.....	42
Figure 43. Velocity Volume Rendering view 2 Model 2	42
Figure 44. Velocity Volume Rendering view 3 Model 2	42
Figure 45. Pressure Contour Left Nostril.....	43

Figure 46. Pressure Contour Right Nostril.....	43
Figure 47. Pressure Outlet in model 2.....	43
Figure 48. Velocity contour on right nostril model 2	44
Figure 49. Velocity contour on left nostril model 2	44
Figure 57. Residuals plot model 3	45
Figure 58. Velocity volume rendering in model 3 view 2.....	45
Figure 59. Pressure contour left nostril model 3	46
Figure 60. Pressure Outlet Contour in model 3.	46
Figure 61. Velocity contour on left nostril model 3	47
Figure 62. Velocity streamline model 3.	48
Figure 63. Residuals plot model 4	49
Figure 64. Velocity volume rendering model 4.....	49
Figure 65. Velocity stream line model 4.....	50
Figure 66. Calculating the cell Orthogonalityl.....	54
Figure 67. Calculating the aspect ratio.....	55
Table 1. Created name faces.....	18
Table 2. Mesh type.....	18
Table 3. Cell size of the first mesh.....	28
Table 4. Size of the second mesh	29
Table 5. Size of the third mesh.....	30
Table 6. Size of fourth mesh.....	31
Table 7. Cell size of the fifth mesh	32
Table 8. Size of the sixth mesh.	33
Table 9. Size of the seventh mesh.....	34
Table 10. Size of the eight mesh	35
Table 11. Mesh independence study.	36
Table 12. Boundary conditions set model 1.....	37
Table 13. Boundary conditions set model 2.....	37
Table 14. Boundary conditions set model 3.....	37
Table 15. Boundary conditions set model 4.....	38
Table 16. Area average pressure in model 2.....	43
Table 17. Air mass flow rate entering on the nostrils in model 2	44
Table 18. Comparison of model 1 -2 of the air mass flow rate inlet on the nostrils.	44
Table 19. Comparison of air mass flow rate inlet of model 3 with model 1.	48

1. OBJECTIVE¹

The following project is committed to study the air flow behaviour of human breathing in the nasal cavity by using a computational fluid dynamics (CFD) simulating software, ANSYS Fluent. The development of the research will require the accomplishment of different steps. First of all, the file of the nasal geometry will be set to carry out the simulations in ANSYS Fluent. To set the file, it will be needed to achieve a proper mesh which provide consistent independent results. After obtaining a valid mesh, different real situations will be simulated: normal human breathing, strong conditions of human breathing like the action of sniffing drugs and lastly the particle's injection. The aim of these simulations is to obtain an accurate description of the airflow behaviour in order to know which areas of the nasal cavity are more exposed to the drug effects. From this study, future research can be developed to maximize the nasal drugs delivery in some locations by varying the formulation of the drug or the administration technique.

2. INTRODUCTION

2.1. Neurodegenerative diseases

In the last years, there is an increased interest in the study of the olfactory epithelium (OE) due to neurological medical reasons. The OE lies on the roof of the nasal cavity and it is the part of the olfactory system directly responsible for detecting odors. Study of OE is considered the high interest for the development of brain medicine due to it is the most proximal axonal area of the human brain. Some studies have demonstrated that the loss of smell has a direct link with the appearance of neurodegenerative diseases. Therefore, some cases could be treated before motricity deficiency signs and loss of memory appears. This medical evidence is motivating the interest for a deeper study of nasal structure, specifically the OE area. The structure of this connection is represented in the figure 1. (CE' DRIC GIRERD, 2018)

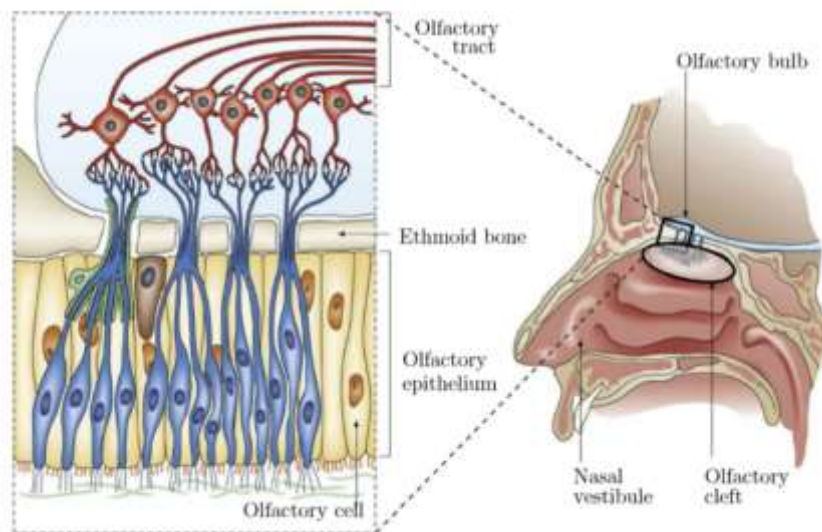


Figure 1. Olfactory mechanism and the related anatomy, with a global view of the nasal cavity on the right and a detailed view of the tissues that cover the roof of the olfactory cleft on the left.

Besides the fact that the diagnosis of neurodegenerative diseases such as Alzheimer and other dementias have increased a 66% from 2005 to 2030. In the case of Alzheimer disease, every 3 seconds a person in the world develops the disease. In 2018, there were around 50 million people on the globe living with Alzheimer and the number of diagnosed cases will almost double every 20 years, reaching 131,5 million by 2050.

Regarding the money Alzheimer moves, it can be considered as a big economy. The total estimated cost of Alzheimer in the world was US\$ trillion in 2018, which represents 1.1% of global GDP and this figure is estimated to reach the US\$ 2 trillion by 2030. This cost takes into account informal care provided by family, direct costs of social care provided by community care professionals and in residential home, and the direct costs of medical care.

Another highlighted figure, it is the number of diagnosed dementia is increasing faster in developing countries. 58% of patients are living in low and middle countries such as China, India, and their south Asian and western Pacific neighbours. These statistics are represented in figure 2. (Alzheimer's Disease International (ADI), 2018)

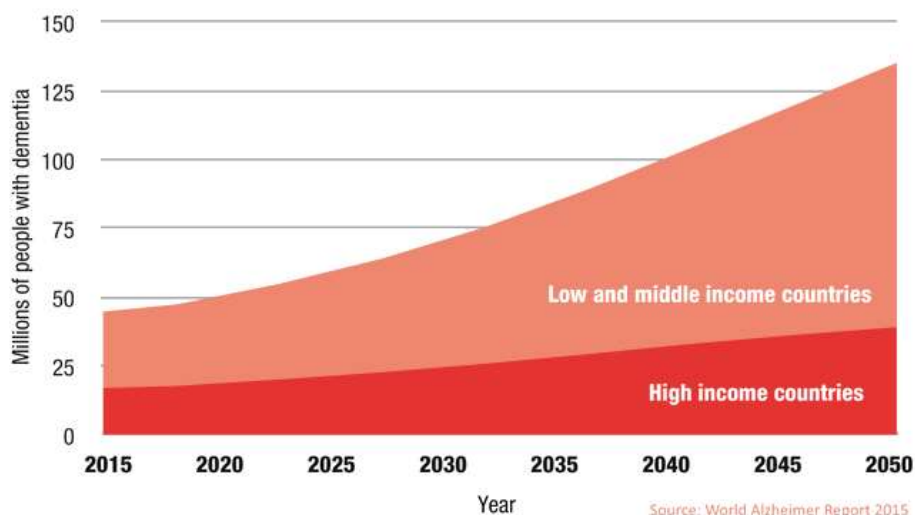


Figure 2. Number of people with dementia in low and middle income countries compared to high income countries

Given these alarming figures, scientific community is more committed to find cure to this disease or move forward in the current techniques used.

Currently, the treatment remains limited to a few conventional oral medications (approved by FDA). These are mainly acting superficially from mild to the moderate AD. The therapeutic efficacy of the drug is not only affected by its reduced concentration in the brain owing to the existence of blood-brain-barrier (BBB) but also due to its low brain permeability.

Presently, there are two categories of drugs used for the treatment of AD: one is symptomatic which is destined to alive the symptoms. They are called AChE3 inhibitors like rivastigmine, galantamine, donepezil. While the other one acts on the specific site or physiological factor of the AD.

Although almost all the treatments of the Alzheimer Disease and other CNS disorders use the oral and parenteral routes to administrate the drug, it has been seen that this method of injection reduces the efficacy and potency of the drug therapy. This occurs because of the existence of Blood-brain-barrier (BBB), whose function is protect the brain from toxic substances, bacteria and viruses. The BBB also filters the entrance of drug molecules such as phytoconstituents, proteins, peptides and other large substances not allowing the drugs reach the brain.

Moreover, the oral and parental route involve a lower drug bioavailability in the brain due to the metabolism and enzymatic degradation when the drug is injected by oral via and wastage of the drug through systemic clearance when the drug is injected by oral and parental route. (Mukta Agrawala, 2018)

2.1 Nasal Anatomy

As the nasal geometry is the objective of the present project, it is necessary to explain in detail its geometry. As Figure 3 illustrates, the geometry of the nasal cavity can be classified into three regions:

- i) Vestibular region. Also, it is called squamous mucosa. It is the entrance of the nasal cavity from the nostrils. In this vestibule, which is characterized by the mucus and hairs, the pass of outside particles is limited.
- ii) Respiratory region. After crossing the vestibular region, the respiratory region starts. It is the largest area of the nasal cavity covering around 130 cm² areas, where protuberances named “turbinates” are apparent with inferior, middle and superior turbinates. The respiratory region is vascularized with blood vessels and also contains the trigeminal sensory neurons. The drug pass to the systemic circulation through the blood vessels while the trigeminal neurons facilitates the drug transport to the cerebrum of the brain.
- iii) Olfactory region. The olfactory region, also called olfactory mucosa, is located in the roof of the nasal cavity, underneath the cribriform plate of ethmoid bone. It involves four kinds of cells: supporting cells, microvillar cells, basal cells, olfactory receptor neurons in the majority with a small portion of trigeminal neurons. The olfactory mucosa is the only place in the body where the central nervous system is directly connected to the external environment, thanks to the olfactory nerves.

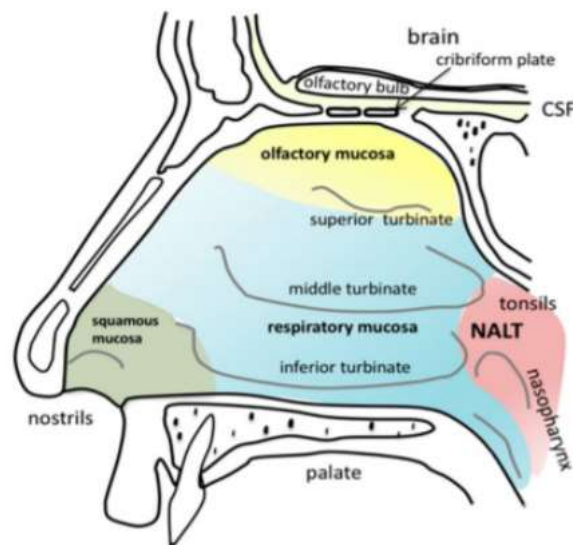


Figure 3. Anatomy of the human nasal cavity (NALT: Nasopharynx-associated lymphatic tissue)

The nasal volume is around 15 mL, its length is approximately 12-14 cm and presents a pH range of 5.5- 6.5. The temperature in the nose is slightly below the human body temperature and ranges between 33 and 35°C. Thanks to its respective mucosa, the nose allows a molecule to be transferred to other anatomical sites. (L. Salade, 2019)

2.2 Intranasal drug delivery

In this context, some new administration techniques are being studied. Intranasal delivery overcomes some of the limitations that oral and parental techniques involve. The nasal cavity permits a direct connection to the brain thanks to the OE as shown in Figure 1 and Figure 3. Some of the benefits of a nose to brain drug delivery presents: it is a faster delivery of the drug and a higher bioavailability of the drug in the brain due to the drug does not have to cross the Blood Brain Barrier in this route. Moreover, it is a safe way to get the central nervous system because it is a non-invasiveness technique.

The nasal drug delivery follows the next mechanism: the drug molecules can reach the brain by two ways: Neuronal pathway where most of the drug amount is transferred and through systemic circulation. The figure 4 illustrates the mechanism.

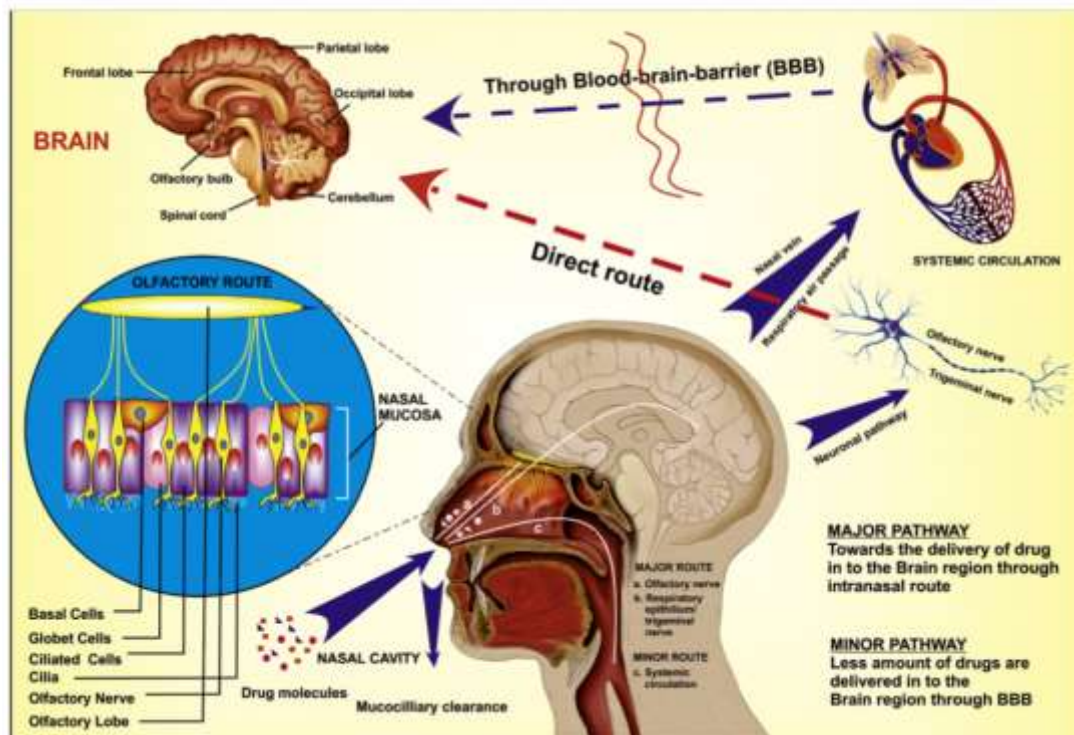


Figure 4. Mechanisms of drug transport from the nasal cavity to the brain

When the drug molecule enters into the nasal cavity, it firstly experiences the mucociliary clearance in the vestibular region. Afterward, the drug moves to the posterior region of nasal cavity where it interacts with the respiratory region and olfactory region. In this region, the drug transport from the nasal cavity to the brain takes place via different mechanisms including; olfactory nerve pathway, trigeminal nerve pathway, lymphatic and vascular pathway and CSF. There is a massive contradiction among the scientists working in nose-to-brain drug delivery, about the exact mechanism of drug transport to the brain. It may follow a single route of drug transport or combination of pathways mentioned above.

The selection of drug transport pathway depends upon the nature of the drug, the formulation parameters, the physiological condition, the type of delivery devices, etc. (Mukta Agrawala, 2018)

2.3 Constraints on the nasal drug delivery.

On the other hand, Intranasal delivery presents some drawbacks. The complex geometry of the nose is not easy to cross and presents narrow hollows to move through. Besides the action of the nasal mucosa and mucociliary clearance do not allow the drug permeation.

To meet nasal-specific criteria, the formulator has to complete a plethora of tests, in-vitro and ex-vivo, to assess the efficacy and tolerance of a new drug-delivery system. Moreover, depending on the desired therapeutic effect, the delivery of the drug should target a specific pathway that could potentially be achieved through a modified release of this drug.

The nose is one of the first defence barriers against external toxins and microbes. It is therefore equipped with a rapid mucociliary clearance, in which the mucus is displaced at a rate of 5 mm/min, with a turnover of 15-20 min. This justifies the use of mucoadhesive agents to increase the drug residence time in the nose. The barrier function is also ensured by the presence of multiple nasal enzymes, macrophages, humoral mechanisms, etc. Another anatomic relevant parameter of the nasal mucosa is the presence of tight junctions that limit permeability through the mucosa. These effective defence mechanisms result in a rapid elimination and poor permeability of deposited particles. Therefore, effective formulation strategies have to be developed to overcome such limitations.

Hence specially designed intranasal devices, mucoadhesive system, surface-engineered nanocarriers, etc. are used to reduce the mucociliary clearance of drug. (L. Salade, 2019)

3. MATHEMATICAL MODEL (EQUATIONS AND BOUNDARY CONDITIONS).

After establishing the modelling goals, the starting point of any computational flow-modeling project is to develop a mathematical model (equations and boundary conditions) to describe the relevant flow phenomena. This involves a rigorous analysis of fluids and type of flow under consideration. For Newtonian² fluids, the knowledge of fluid viscosity is sufficient to develop the governing fluid dynamic equations. In our case, human breathing, we are dealing with air which clearly behaves as a Newtonian fluid.

To select the adequate model is needed to know other properties of the air:

- Compressible/incompressible.
- Laminar/turbulent.
- Isothermal/non-isothermal;
- Single phase/multiphase.

The flow behaviour of human breathing let consider the air as an incompressible fluid. Therefore, Navier-Stokes equations are valid to describe the flow behaviour. In our case, the two first models clearly behave as a laminar flow. The sniffing case reaches air velocities in some areas of the nose that makes the flow behaves as a turbulent flow. But, it will run like a laminar model to reduce the time solving and to simplify the model. In resume, the four models can be considered as laminar. The cases are going to be supposed like steady and energy equation will be neglected a priori.

The four models will be considered as a single phase. The particle's injection case could be considered as multiphase system, but particle's velocity will be considered equal to the air velocity what means the relative velocity is 0. Therefore, it can be treated as a single phase.

Development of generic Flow Models

It is essential to know the mathematic of the flow we want to model. Most of the following cases run are governed by the equations of a single-phase flow model. The conservation equation is applied to 3 variables: mass, momentum and energy.

Conservation of Mass

The mass conservation equation for species k can therefore be written:

$$\frac{\partial}{\partial t}(\rho \cdot m_k) + \nabla \cdot (\rho \cdot U \cdot m_k) = -\nabla \cdot (j_k) + S_k \quad (\text{equation 1})$$

$$t = \text{time}$$

$$\rho = \text{fluid density};$$

² A Newtonian fluid is a fluid in which the viscous stresses arising from its flow, at every point, are linearly proportional to the local strain rate—the rate of change of its deformation over time. That is equivalent to saying those forces are proportional to the rates of change of the fluid's velocity vector as one moves away from the point in question in various directions

$m_k = \text{mass fraction of species};$

$U = \text{fluid velocity}$

The first term on the left-hand side of this equation represents accumulation of species k in volume element and the second term represents change in species mass fraction due to convection. The first term on the right-hand side represents the change in species mass fraction due to diffusive fluxes, j_k . S_k is the source of species k (net rate of production per unit volume) which can be cut out since there is no reaction.

$$\frac{\partial}{\partial t}(\rho \cdot m_k) + \nabla \cdot (\rho \cdot U \cdot m_k) = -\nabla \cdot (j_k) \quad (\text{equation 2})$$

Conservation of Momentum

Application of the law of conservation of momentum yields a basic set of equations governing the motion of fluids, which are used to calculate velocity and pressure fields. The governing equations can be written:

$$\frac{\partial}{\partial t}(\rho \cdot U) + \nabla \cdot (\rho \cdot U \cdot U) = -\nabla \cdot \pi + \rho \cdot g + F \quad (\text{equation 3})$$

Mapping these Models onto CFD Solver

Select numerical method and solver to approximate the differential equation by a system of algebraic equations in terms of the variables at some discrete locations in space and time (called discretization method).

There are many such methods; the most important are finite difference (FD), finite volume (FV) and finite element (FE) methods. In our case, it is going to be used the Finite Volume (FV).

Finite Volume (FV) method.

FV uses the integral form of the conservation equations as its starting point to ensure global conservation. The solution domain is again divided into number of computational cells. The differential equation is integrated over the volume of each computational cell to obtain the algebraic equations. Variable values are stored at the cell centre values. Surface and volume integrals are approximated using suitable quadrature formulae. As a result, one obtains an algebraic equation per computational cell, in which a number of neighbouring cell centre values appear as unknowns. The FV methods can accommodate any type of grid and is, therefore, quite popular with engineers.

4. SET-UP THE MODEL IN ANSYS

In the next section, it explains how the model has been set up in the software ANSYS FLUENT.

4.1. Import and edit the STL file

The stl file geometry has been imported as 1 volume and 1 surface by the option “Import file”. Secondly, the surface area has been divided in 4 different faces: two nostrils, the mouth connection and the rest of the nasal body by using ANSYS Spaceclaim. ANSYS Spaceclaim is an editor software for files which have been transferred from softwares like Solidworks.



Figure 5. Display of the nose.

4.2. Meshing

Once the nose file has been imported and edited. The different created faces should be named. In our model, the faces are named as next table indicates:

Table 1. Created name faces.

Nasal Part	Name selection
Left Nostril	Velocity-Inlet-Left
Right Nostril	Velocity-Inlet-Right
Mouth connection	Pressure Outlet
Nasal body	Body

Then, a computational mesh should be generated throughout the flow volume. 3rd step is mesh the geometry for the CFD analysis with the complement ANSYS Meshing. By choosing the proper mesh type will improve the mesh generation efficiency.

During the meshing process many parameters have to be chosen:

Table 2. Mesh type

Mesh type	
Algorithm	Patch conforming
Method	Tetrahedrons

Cell size (mm)	0,5
----------------	-----

As the table above indicates, it has been chosen the algorithm patch conforming and the method tetrahedrons among the different options to mesh a geometry.

The advantages of this method regarding the others is the ease to mesh more complex geometries like is the case of the present nasal geometry. Moreover, the mesh quality obtained is better with tetrahedral method mesh than others like hexahedral.

Another relevant parameter, it is the element size of our cells. Because it will define the CPU time and the accuracy of the results. In first simulation, cell size has been defined in 0,5 mm.

After meshing, the total obtained elements are:

NODES	826088
ELEMENTS	2294438

Figure 6. Nodes and elements of first mesh.

The details of the obtained mesh are represented in the figure 7:

Details of "Mesh"	
+ Display	
- Defaults	
Physics Preference	CFD
Solver Preference	Fluent
Element Order	Linear
<input type="checkbox"/> Element Size	0,5 mm
Export Format	Standard
Export Preview Surface Mesh	No
- Sizing	
Use Adaptive Sizing	No
<input type="checkbox"/> Growth Rate	Default (1,2)
<input type="checkbox"/> Max Size	Default (1, mm)
Mesh Defeaturing	Yes
<input type="checkbox"/> Defeature Size	Default (2,5e-003 mm)
Capture Curvature	No
Capture Proximity	No
Bounding Box Diagonal	122,49 mm
Average Surface Area	0,32416 mm ²
Minimum Edge Length	2,6577e-003 mm
- Quality	
Check Mesh Quality	Yes, Errors and Warnings
<input type="checkbox"/> Target Skewness	Default (0.900000)
Smoothing	High
Mesh Metric	None
- Inflation	
Use Automatic Inflation	Program Controlled
Inflation Option	Smooth Transition
<input type="checkbox"/> Transition Ratio	0,272
<input type="checkbox"/> Maximum Layers	5
<input type="checkbox"/> Growth Rate	1,2
Inflation Algorithm	Pre
View Advanced Options	No
+ Assembly Meshing	
- Advanced	
Number of CPUs for Parallel...	Program Controlled
Straight Sided Elements	
Rigid Body Behavior	Dimensionally Reduced
Triangle Surface Mesher	Program Controlled
Topology Checking	Yes
Pinch Tolerance	Default (4,5e-003 mm)
Generate Pinch on Refresh	No

Figure 7. Details of the first mesh with a cell size of 0,5 mm.

Details of "Patch Conforming Method" - Method	
- Scope	
Scoping Method	Geometry Selection
Geometry	1 Body
- Definition	
Suppressed	No
Method	Tetrahedrons
Algorithm	Patch Conforming
Element Order	Use Global Setting

Figure 8. Details of the selected Patch Conforming Method.

4.3. Set-Up

After obtaining the mesh for nasal geometry, it is required the set-up of a CFD analysis using ANSYS Fluent.

In the set-up step, different aspects will be defined such as the unit domain, the physics set-up, but the most important the boundary conditions.

4.3.1. Set-up domain

The length units selected is mm.

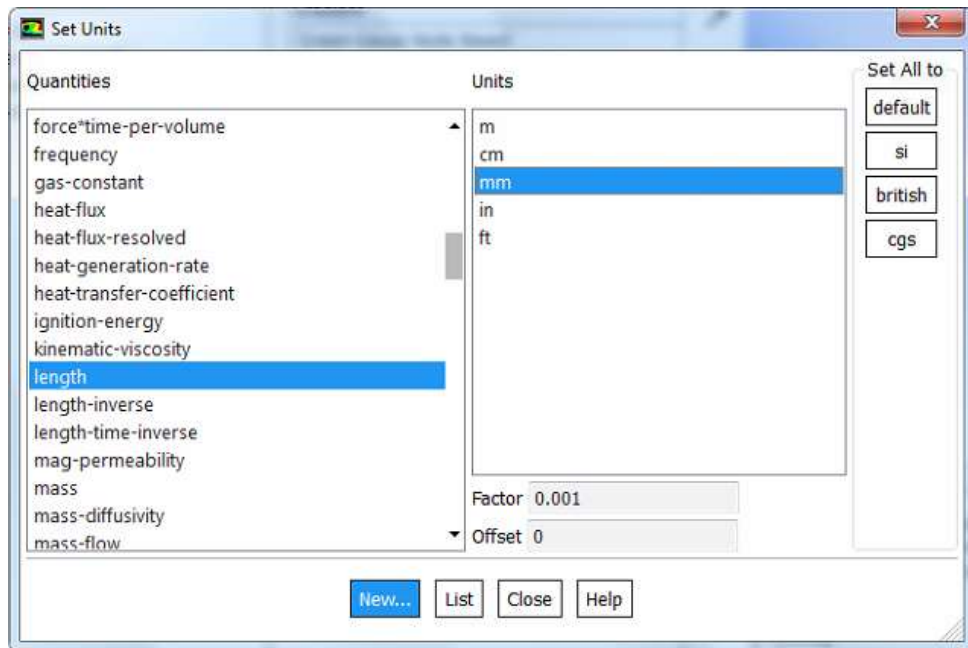


Figure 9. Set units

4.3.2. Set-up Physics

In the physic of the model, several parameters should be defined as figure 10 indicates:

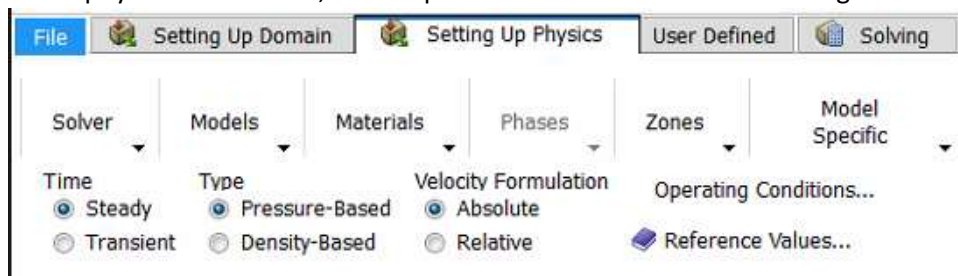


Figure 10. Setting up physics parameters.

4.3.3. Models

The set up model will define the mathematic equations used to calculate the flow behaviour. In our case, viscous model will be selected and the energy model will be disabled since the heat transfer will be neglected.

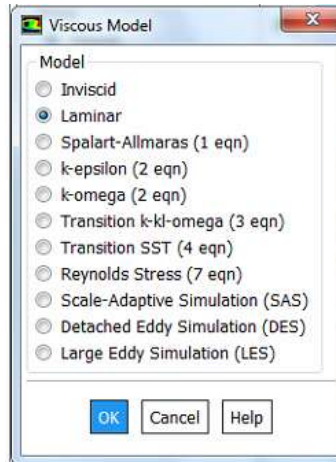


Figure 11. Selected model in set up physics.

Once inside the viscous model, the Laminar model will be selected since calculated Reynolds number gives a result below 2100.

$$Re = \frac{\rho \cdot v_s \cdot D_H}{\mu}$$

ρ : air density at 15 °C , 1.225 kg/m³

v_s : velocidad característica de inspiración

D : hydraulic diameter nasal cavity

μ : air dynamic viscosity at 15°C ($1.81 \cdot 10^{-5} \cdot \frac{kg}{m \cdot s}$)

According to experimental data, it is known that the human breathing capacity is around 250 ml/s taking into account both lungs. Then, to calculate the characteristic velocity of inspiration:

$$Q_{left} + Q_{right} = 250 \text{ ml/s}$$

$$Q_{left} = Q_{right} = 125 \frac{ml}{s} = 125 \cdot 10^{-6} m^3/s$$

$$v_{left} = \frac{Q_{left}}{A_{left}} = \frac{125 \cdot 10^{-6} m^3/s}{87,142 \cdot 10^{-6} m^2} = 1,43 m/s$$

$$v_{right} = \frac{Q_{right}}{A_{right}} = \frac{125 \cdot 10^{-6} m^3/s}{143,85 \cdot 10^{-6} m^2} = 0,869 m/s$$

In order to be sure, it is going to be supposed a velocity of 1,5 m/s taking into account that the nasal cavity narrows as the flow progresses.

Hence, the calculation of Re number:

$$Re = \frac{\rho \cdot v_s \cdot D_H}{\mu} = \frac{1,225 \cdot 1,5 \cdot 0,0144}{1,81 \cdot 10^{-5}} \cong 1342 \lll 2100 \quad \text{LAMINAR}$$

$$D_H = \frac{4 \cdot Area}{Perímetro} = \frac{4 \cdot 143,85 \cdot 10^{-6}}{0,04} = 0,0144$$

4.3.4. Materials.

Air will be selected from the Fluent Database such as Fluent Fluid Material flowing through the nasal cavity. The air of the database has the properties at the 20°C and 1 atm as it is shown in the figure 14:

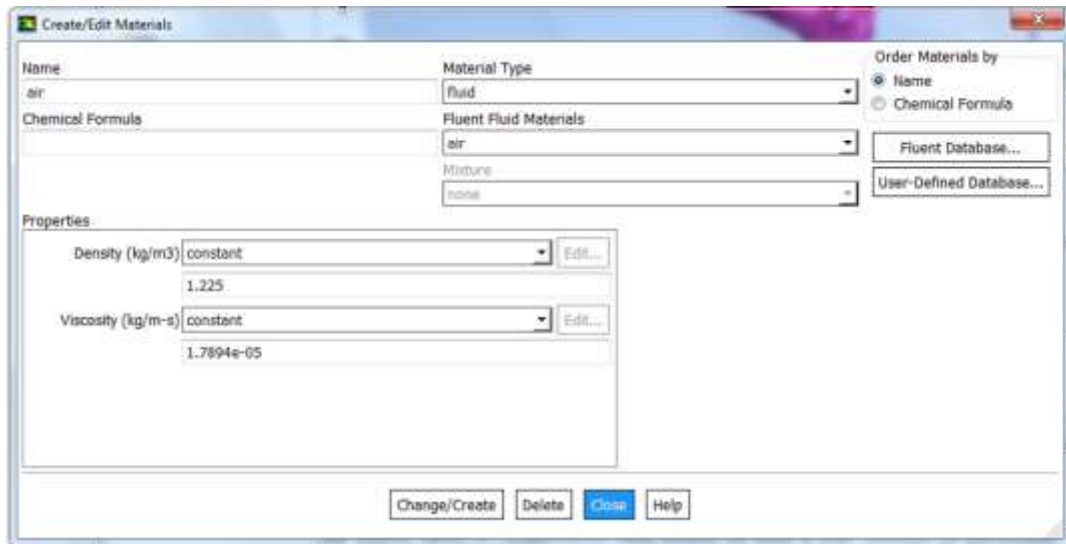


Figure 12. Create materials.

4.3.5. Zones

In zones section, zone conditions and boundary conditions must to be defined.

In the cell zone, the phase of the zone (solid or fluid) is specified. In our model, the zone phase will be fluid as figure 13 indicates.

The Boundary conditions are essential components of a mathematical model. They direct the motion of flow which leads to a unique solution. In ANSYS FLUENT we are familiar with standard boundary conditions such as inlet, outlet, wall, symmetry etc.

In the first simulated model, it has been defined the boundary conditions of figure 14 indicates.

To calculate the inlet mass flow rate per nostril, it is just needed multiply the air flow per air density:

$$m_{air}^{\dot{}} = Q_{air}^{\dot{}} \cdot \rho_{air}$$
$$m_{air}^{\dot{}} = 125 \cdot 10^{-6} \frac{m^3}{s} \cdot 1.225 \frac{kg}{m^3} = 153,125 \cdot 10^{-6} kg/s$$



Figure 13. Cell zone conditions set up.

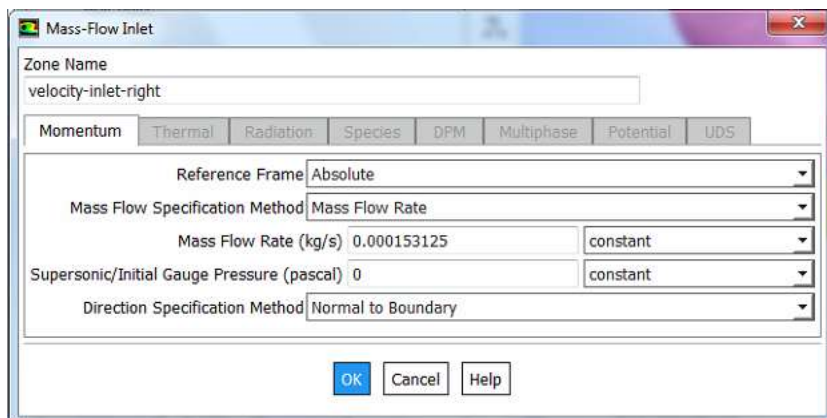
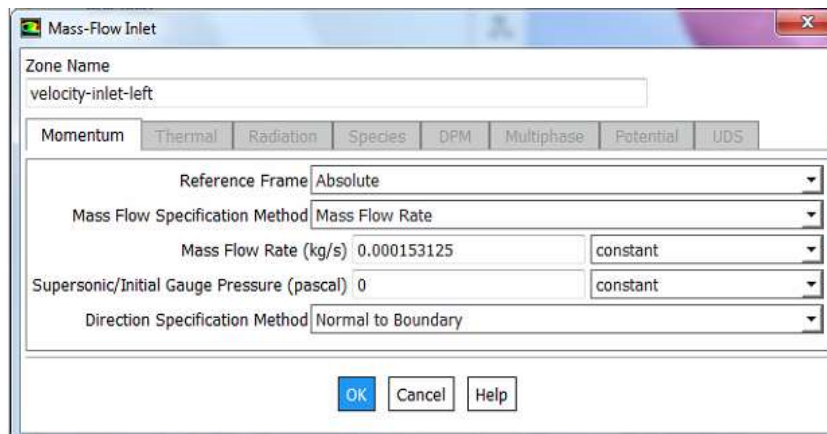


Figure 14. Boundary conditions inlet set up

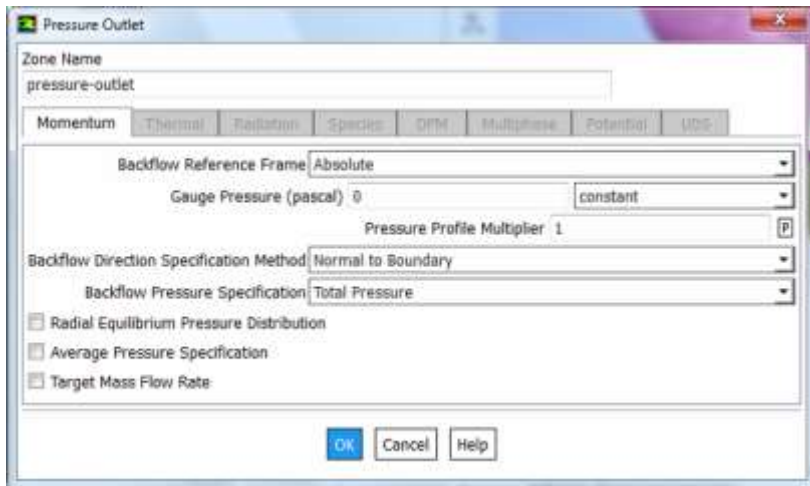


Figure 15. Boundary conditions outlet set up.

4.4. Solution

In the Solving section, it is set up and run the calculation. In this section, it is selected the solution method is going to be used to solve the simulation. In our case, it has been chosen the next method:

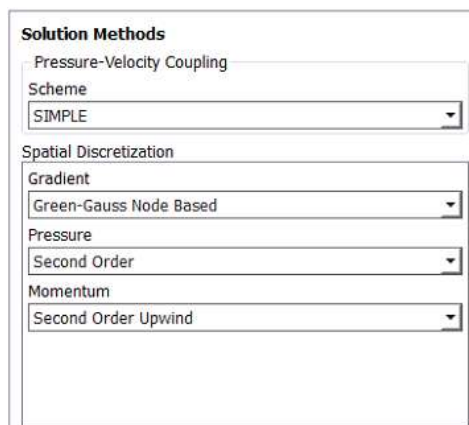


Figure 16. Solution Method set up.

Then, the residuals have been fixed in 10^{-6} .

The convergence results obtained for the first simulation are the next ones:

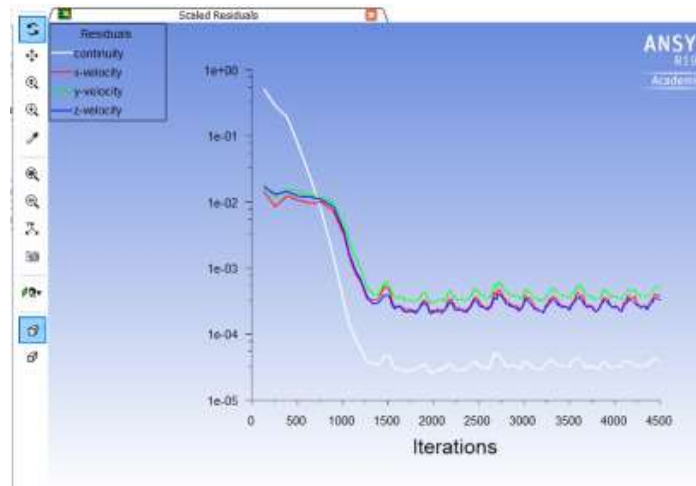


Figure 17. Residuals for cell size of 0,5 mm.

They can be considered enough good because the residuals are under 10^{-3} .

4.5. Post-processing results

After running the simulation, the last step is analysing the results. In the post processing section different tools can be used to an easy visualization of different variables.

4.5.1. Contour plane

First one used, it is the contour plane. Different planes have been defined by 3 points method or by 2 axes and a distance which will intersect the nasal cavity. These planes display the value of the desired value.

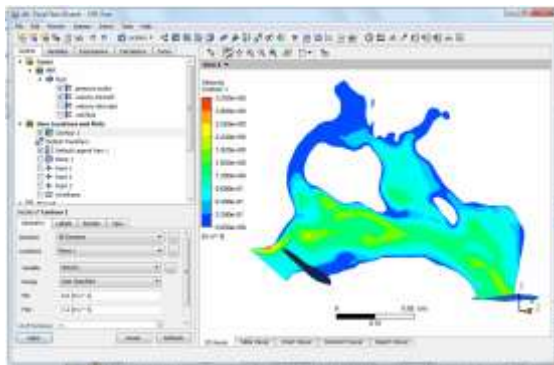


Figure 19. Velocity contour right nostril

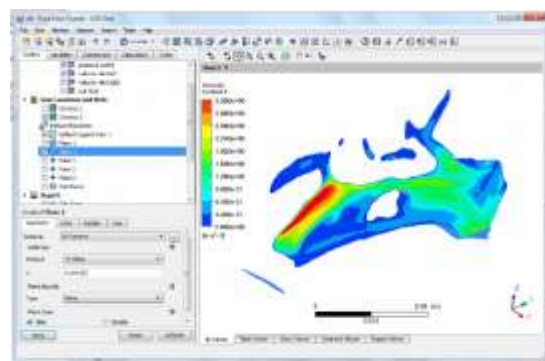


Figure 18. Velocity contour left nostril

4.5.2. Volume Rendering

The second tool used is the rendering volume. This tool renderise the velocity field in the 3D nasal geometry. This tool is very useful to obtain a general overview of the velocity airflow breathing. In the following image, it can be appreciated how the airflow velocity is higher in the left nostril than in the right nostril. These simulations accomplish with the theoretical calculations. This velocity difference is due to the fact the left nostril area is smaller than the right nostril.

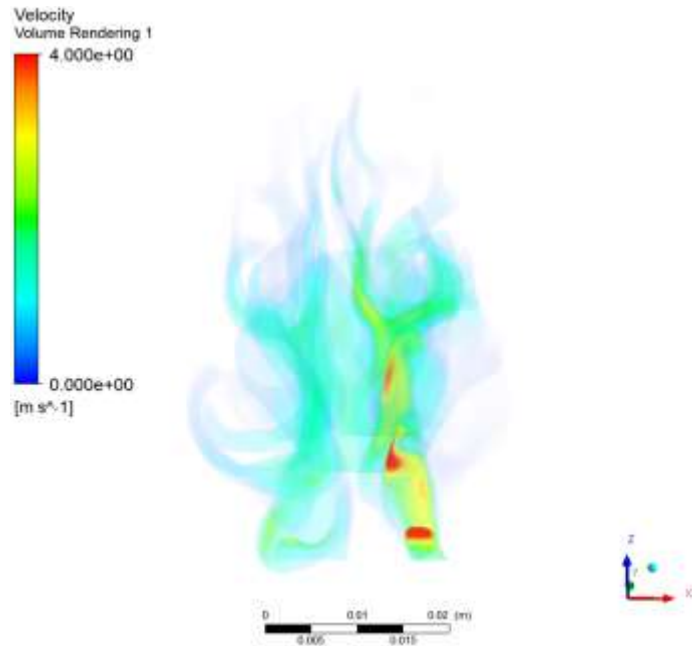


Figure 20. Volume rendering of the airflow velocity

Another conclusion can be extracted from the post processing results: airflow velocity in the left sinus is around 0 m/s. That implies that this part of the nasal geometry does not take high relevance in the airflow behaviour. Hence, it could be neglected in future studies in order to reduce the solving time of the simulation.

4.5.3. Streamline

Thanks to the streamline tool, it can be appreciated the pathway that particles follow in the nasal cavity.

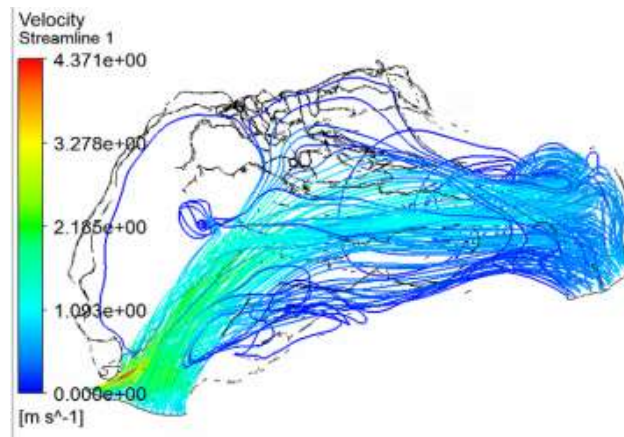


Figure 21. Streamline tool.

5. MESH INDEPENDENCE STUDY.

It is not just enough with checking that the residuals are under certain values to assure that your results are numerically correct. Another study which should be carried out is the independence of the mesh resolution.

If the obtained results are mesh independent means that they do not change as function of the size of the meshing. On the contrary, if we come up with different results for different cell sizes implies that the different mesh represents different physical systems and the discretization is not enough.

One fact to take into account when this study is developed is: the smaller the cell size of the mesh, the more accurate the results. But as a drawback the simulations take longer.

The procedure to do a mesh independence study is the following: First trial will be run and it will be assured that residuals are under certain values. After that, the mesh size will be decreased and results will be analysed. In our case, pressure outlet will be the variable of interest. Once the pressure outlet keeps approximately constant using consecutive mesh sizes it can be confirmed that the mesh is independent.

Pressure outlet will be measured with post-processing tool. A contour plane measures the pressure outlet. It is supposed to be the lowest one. Local range will be set up as an axis, which uses the variable values on the current object at the current time step to set the maximum and minimum range values instead of using global range, which uses the variable values from the results in all domains and all time steps. The time step of interest is the last one.

1st mesh

The first mesh will be defined with a cell size of 0,5 mm.

Table 3. Cell size of the first mesh.

Cell size of 0,5 mm	
Nodes	826088
Elements	2294438

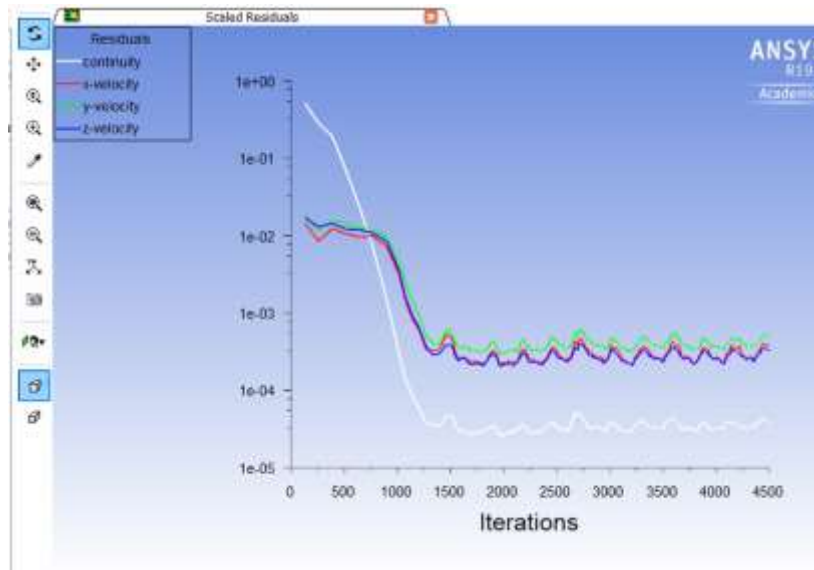


Figure 22. Scaled residuals plot of the first mesh

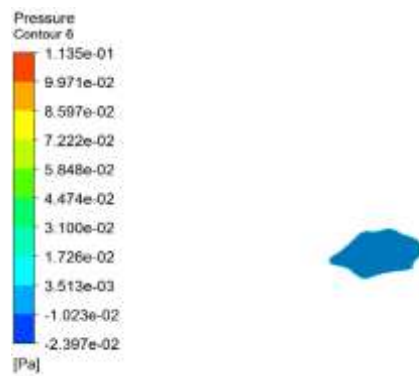


Figure 23. Pressure outlet of the first mesh

The pressure outlet is -0,0239 Pa

2nd mesh

The second mesh will be defined with a cell size of 0,4 mm. But it does not converge.

Table 4. Size of the second mesh

Cell size of 0,4 mm	
Nodes	1267246
Elements	3626195

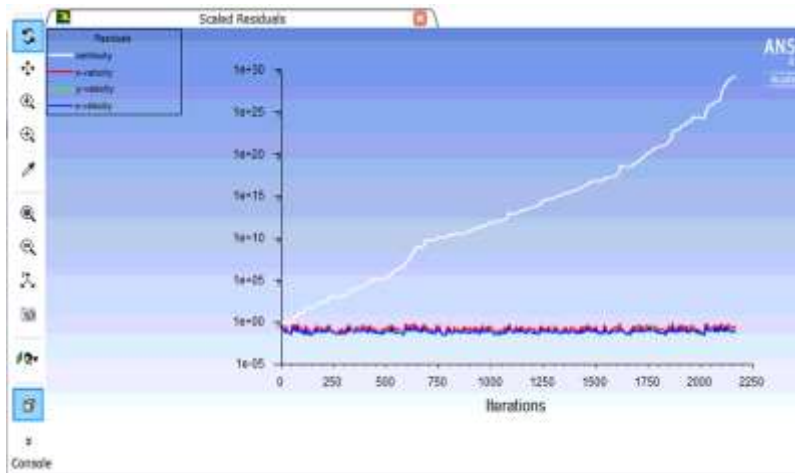


Figure 24. Scaled plot residuals of the second mesh.

Certain cell size makes that the continuity equation does not converge.

3rd mesh

The third mesh will be defined with a cell size of 0,45mm. The running results of this case takes by far the longest time. The residuals results are the following:

Table 5. Size of the third mesh

Cell size of 0,45 mm	
Nodes	1013385
Elements	2875025

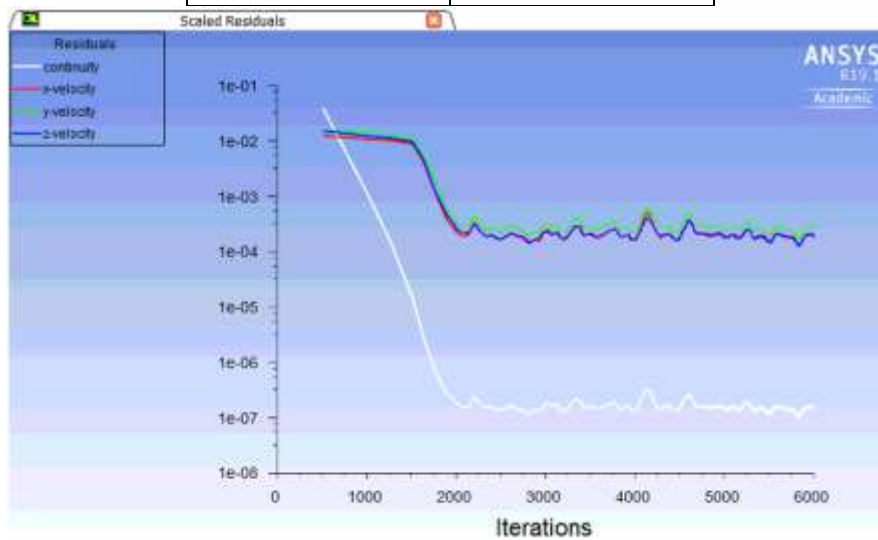


Figure 25. Scaled residuals plot of the third mesh

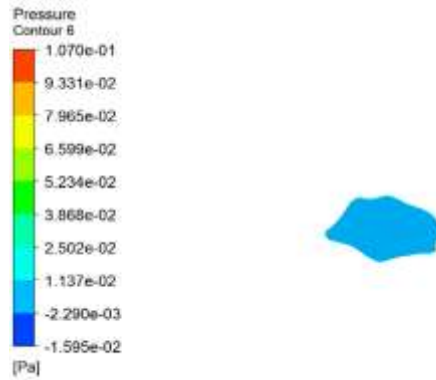


Figure 26. Pressure Outlet of the second mesh

The pressure outlet is -0,01595 Pa

4th mesh

The fourth mesh will be defined with a cell size of 0,43mm. The running results of this case takes by far the longest time. The residuals results are the following:

Table 6. Size of fourth mesh.

Cell size of 0,43 mm	
Nodes	1109061
Elements	3175209

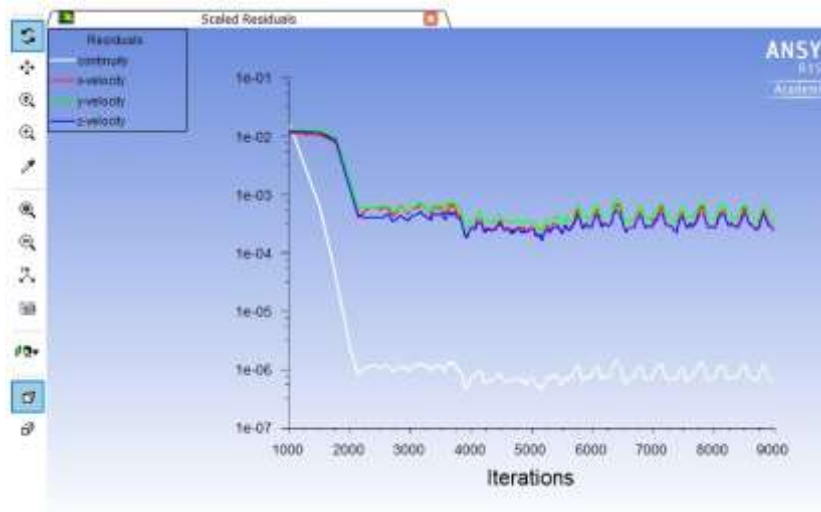


Figure 27. Scaled residuals plot of the fourth mesh

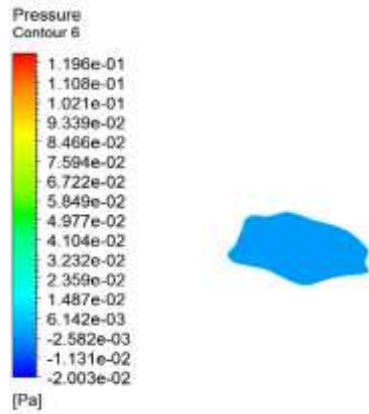


Figure 28. Pressure Outlet of the fourth mesh

The pressure outlet is -0,0200317 Pa

5th mesh

The fifth mesh will be defined with a cell size of 0,35mm. The running results of this case takes by far the longest time. The residuals results are the following ones:

Table 7. Cell size of the fifth mesh

Cell size of 0,35 mm	
Nodes	1666346
Elements	4893469

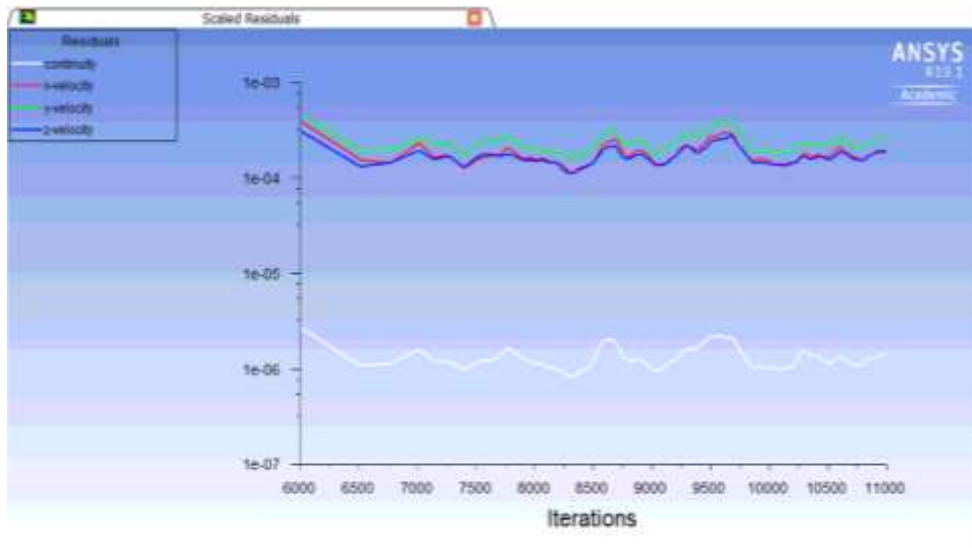


Figure 29. Scaled residuals plot of the fifth mesh.

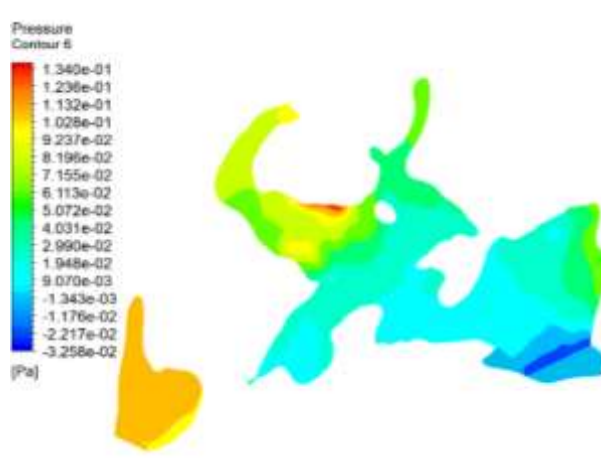


Figure 30. Pressure Outlet contour fifth mesh

The pressure outlet is $-0,03258$ Pa

6th mesh

The sixth mesh will be defined with a cell size of 0,7mm. This the fastest time solving case because the number of cells is the lowest. The residuals results are the following ones:

Table 8. Size of the sixth mesh.

Cell size of 0,7 mm	
NODES	439644
ELEMENTS	1145679

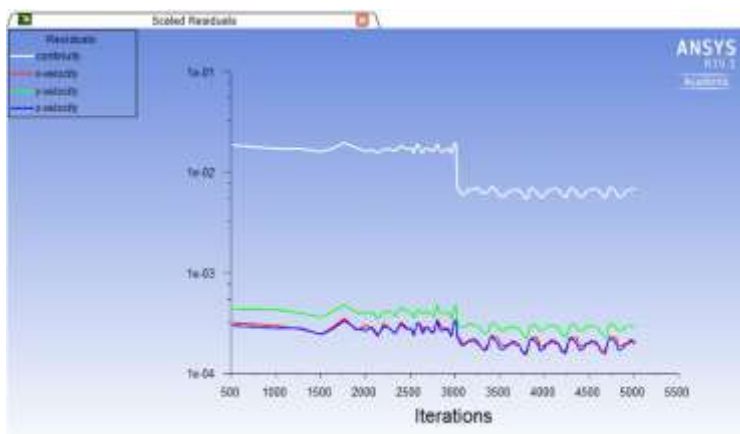


Figure 31. Scaled residuals plot of cell size 0,7 mm

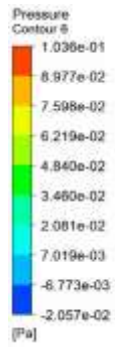


Figure 32. Pressure Outlet contour sixth mesh

The Pressure Outlet is -0,02057 Pa

7th mesh

The seventh mesh will be defined with a cell size of 0,37mm. The residuals results are the following ones:

Table 9. Size of the seventh mesh

NODES	439644
ELEMENTS	4315949

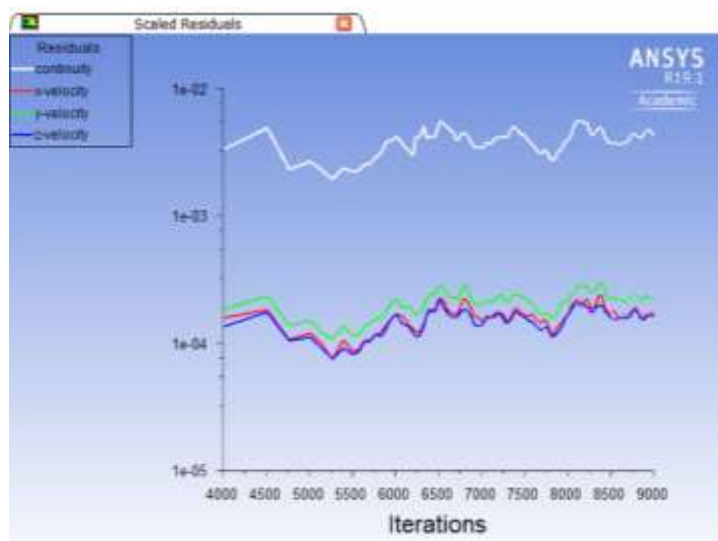


Figure 33. Residuals of cell size of 0,37 mm

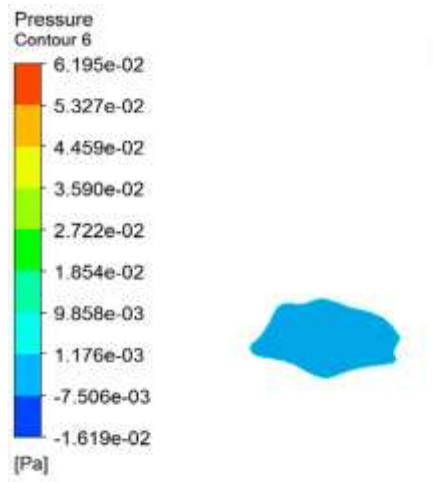


Figure 34. Pressure Outlet contour seventh mesh

The pressure outlet contour of seventh mesh is -0,01619 Pa.

8th mesh

The eight mesh will be defined with a cell size of 0,32mm. The residuals results are the following ones:

Table 10. Size of the eight mesh

NODES	439644
ELEMENTS	4315949

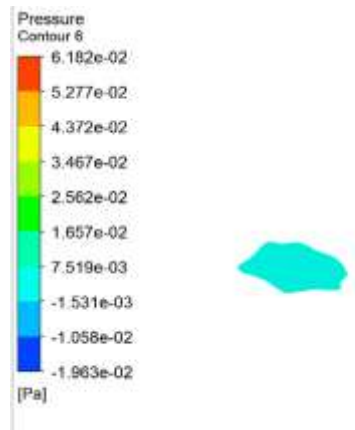


Ilustración 1. Pressure contour eight mesh

Mesh independence study

To facilitate the comparison of the data, all the run cases are exposed in the next table:

Table 11. Mesh independence study.

Cell size (mm)	Number of cells	Pressure Outlet (Pa)	Residuals continuity
0,7	1145679	-0,01697	10 ⁻³
0,5	2294438	-0,0239	10 ⁻⁵
0,45	2875025	-0,01595	10 ⁻⁷
0,43	3175209	-0,0200317	10 ⁻⁷
0,37	4315949	-0,02057	10 ⁻³
0,35	4893469	-0,03258	10 ⁻⁶
0,32	5985550	-0,01963	10 ⁻³

By observing the results, it can be discarded some mesh because their high residuals.

The mesh with cell size 0,7 mm, 0,37 mm and 0,32 mm not should be taken into account since the continuity equation does not go under 10⁻³. That means the mass imbalance error is high. Therefore, results are low accurate.

After analysing the results, we have to make a compromise between accuracy and time-solving. After the comparison of the results, the mesh with a cell size of 0,35 mm is thought to be the most accurate.

6. MODELS

Model 1. Normal conditions breathing imposing the mass flow air.

This case is the one used to set up the model and do the mesh independence study. This model simulates a human breathing in normal conditions.

Table 12. Boundary conditions set model 1

Boundary conditions		
Set	Inlet Mass Flow Rate (kg/s)	0,000153125
	Pressre Outlet (Pa)	0
Calculated	Inlet Pressure (Pa)	5,4138
	Outlet Pressure (Pa)	-0,0325819

Model 2. Normal conditions breathing imposing pressure outlet.

The main function of model 2 is verify the obtained results in model 1. This case is going to be run following an inverse procedure imposing the boundary conditions. In this case, the pressure drop between inlet and outlet is going to be set as a boundary condition and it will be checked that the calculated mass flow rate will be approximately the one set in the first case. Thanks to this simulation, it will be checked that two different set up conduct to similar results.

Table 13. Boundary conditions set model 2.

Boundary conditions		
Set	Pressure Outlet (Pa)	-5,4463819
	Pressure Inlet (Pa)	0
Calculated	Inlet left Mass Flow Rate (kg/s)	

Model 3. Sniffing. Extreme conditions breathing.

Model 3 represents extreme conditions of human breathing. This situation could perfectly depict the action of sniffing drugs such as cocaine in an autonomous way. The model simulates the air sniffing by only the left nasal cavity. To do this, a 2,5 times pressure drop is imposed between the inlet left nostril and outlet. On the other hand, the right nasal cavity is blocked imposing a mass flow rate of 0 kg/s. After running the simulation, some parameters such as the velocity, the pressure and mass flow rate will be compared with case 1.

Table 14. Boundary conditions set model 3

Boundary conditions		
Set	Inlet right nostril Mass Flow Rate (Kg/s)	0
	Pressure Inlet on left nostril(Pa)	0
	Pressure Outlet (Pa)	-16,615955
Calculated	Inlet left Mass Flow Rate (kg/s)	

Model 4. Particle's injection.

Last model simulates the injection of a normal aerosol shoot. It has been needed research about the average flow rate injection in the pharmaceutical market. A mass flow rate of 100 micrograms/s has been set up since most of the aerosols sold in the pharmacy have a dosis of 50 micrograms / pulverisation and considering a pulverisation takes 0,5 seg.

Table 15. Boundary conditions set model 4.

Boundary conditions		
Set	Inlet right nostril Mass Flow Rate ($\mu\text{g/s}$)	100
	Pressure Inlet on left nostril(Pa)	0

7. POST-PROCESSING RESULTS

Model 1. Normal conditions breathing imposing the mass flow air.
The scaled residuals of model 1 are shown in the figure below:

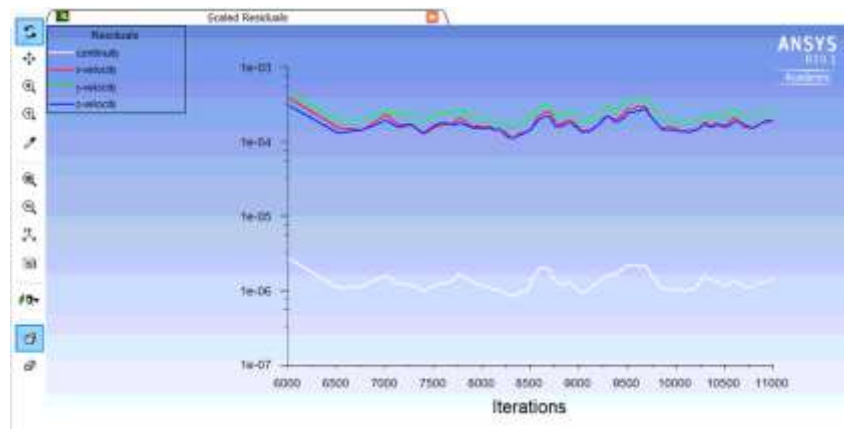


Figure 35. Residuals plot model 1.

Analysing the residuals, the continuity equation is fulfilled since residuals around 10^{-6} are pretty good.

The contour pressure results obtained in the nostrils are the following ones:

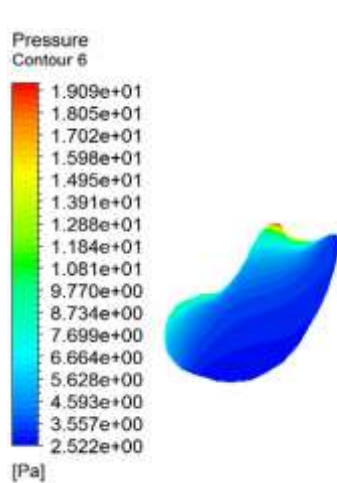


Figure 36. Contour Pressure on Right Nostril

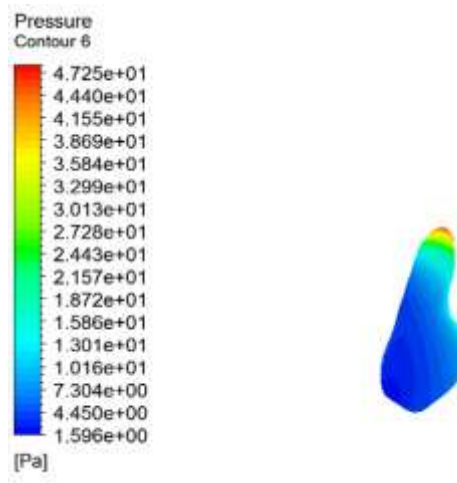


Figure 37. Contour pressure on Left Nostril.

The average pressure on the right nostril and left nostril are calculated with Average Surface tool. This tool helps us to calculate an average value as an inlet pressure in order to calculate the pressure drop in the airflow path between the nostrils and mouth connection.

	Area Average Pressure (Pa)	Area (m ²)

Right Nostril	3.99476	0.000143846
Left Nostril	7.75645	$8.71425 \cdot 10^{-5}$

Total Nostril Area = Area Right Nostril + Area Left Nostril = $2,309885 \times 10^{-4} \text{ m}^2$

$$\text{Average Pressure} = \frac{1.43846 \cdot 10^{-4}}{2,309885 \cdot 10^{-4}} \times 3.99476 + \frac{8.71425 \cdot 10^{-5}}{2,309885 \cdot 10^{-4}} \times 7.75645$$

$$\text{Average Pressure} = 0.62274 \times 3.99476 + 0.377259 \times 7.75645 = 5,4138 \text{ Pa}$$

Then, the difference between the Pressure Inlet and Pressure Outlet is:

$$\Delta P = P_{inlet} - P_{outlet} = 5,4138 \text{ Pa} - (-0,03258 \text{ Pa}) = 5,4463819 \text{ Pa}$$

Model 2. Normal conditions breathing imposing pressure outlet.

The scaled residuals of model 2 are shown in the figure below:

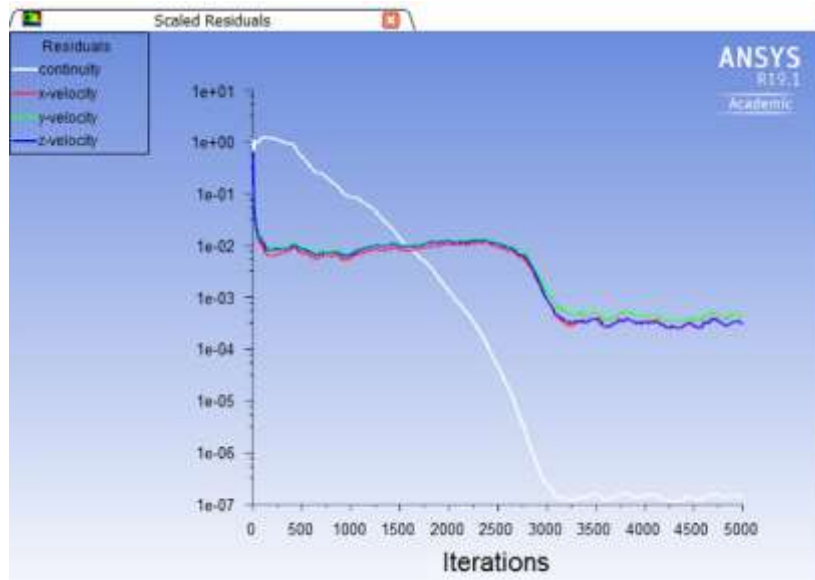


Figure 38. Residuals plot model 2

Analysing the residuals, the continuity equation is fulfilled since residuals values are below 10^{-6} .

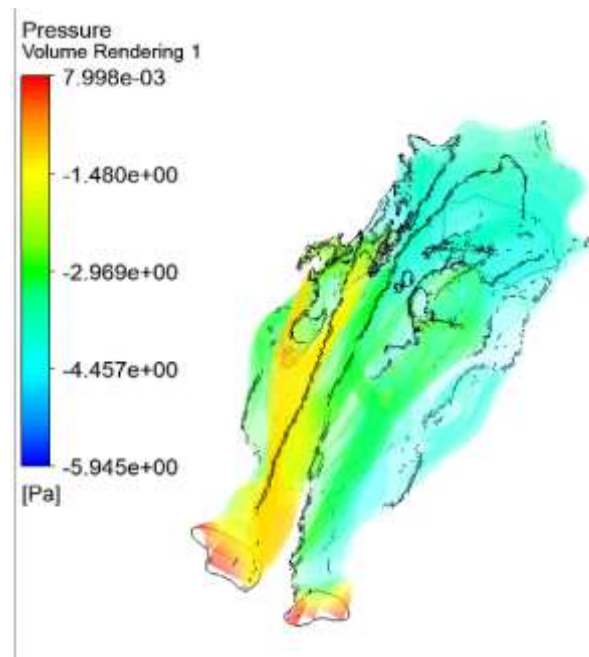


Figure 39. Pressure volume rendering model 2

The value of pressure is not orientative. The important value which should be analysed is the pressure drop between inlet and outlet.

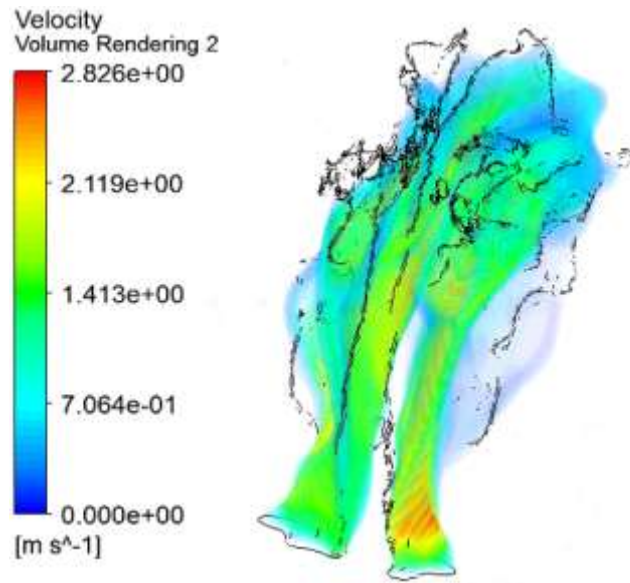


Figure 40. Velocity Volume Rendering Model 2

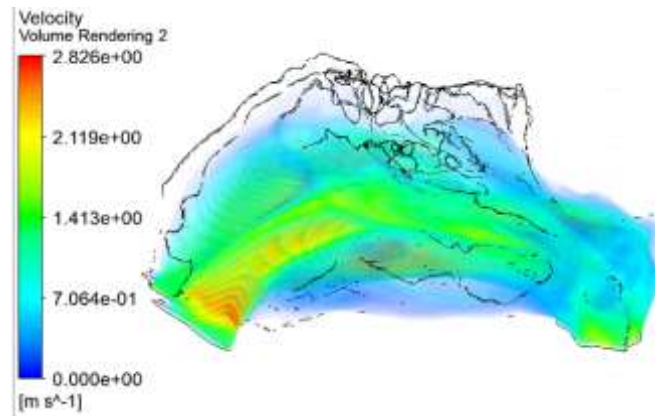


Figure 41. Velocity Volume Rendering view 2 Model 2

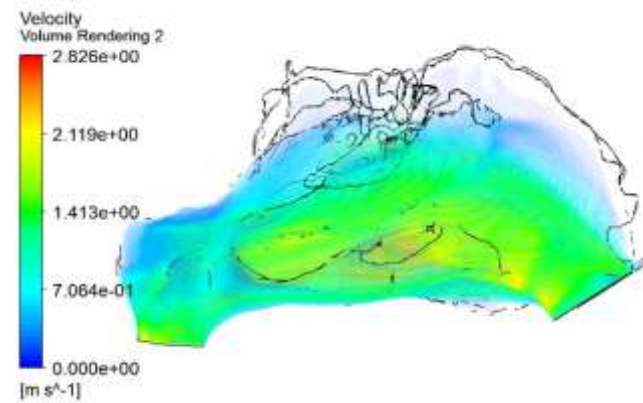


Figure 42. Velocity Volume Rendering view 3 Model 2

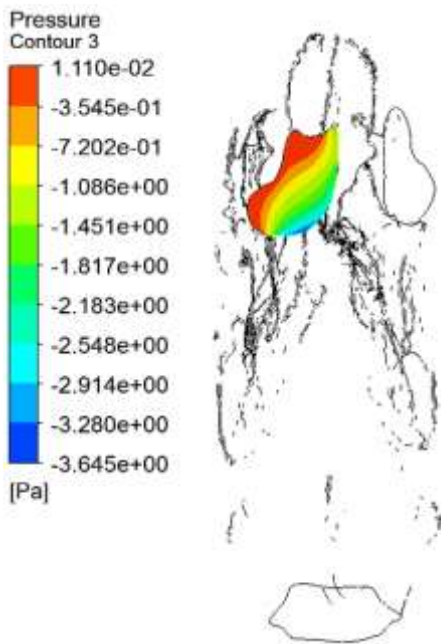


Figure 44. Pressure Contour Right Nostril

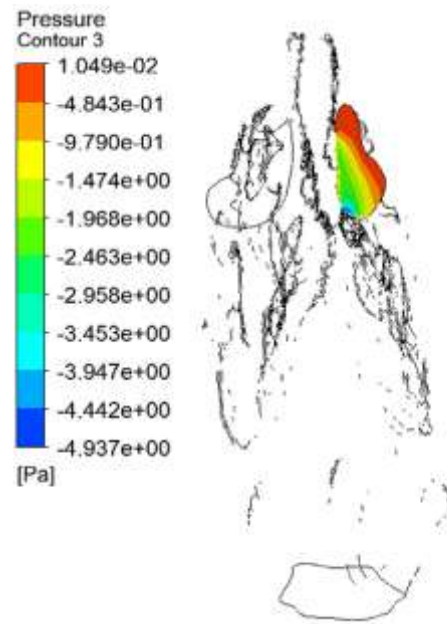


Figure 43. Pressure Contour Left Nostril

The area average pressure in each nostril is:

	Area Average Pressure (Pa)	Area (m ²)
Right Nostril	-1,02021	0,000143846
Left Nostril	-1,13341	8,71425 · 10 ⁻⁵

Table 16. Area average pressure in model 2.

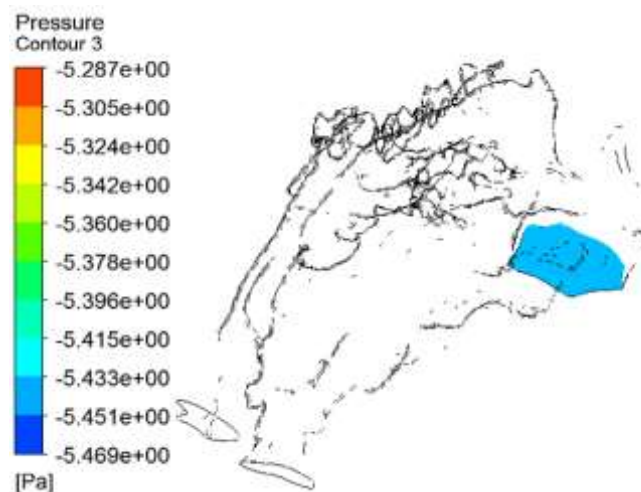


Figure 45. Pressure Outlet in model 2

The area average of pressure outlet is -5.44638 Pa.

So, the pressure drop is around:

$$\Delta P = P_{inlet} - P_{outlet} = -1,05 \text{ Pa} - (-5.44638 \text{ Pa}) = 4,39638 \text{ Pa}$$

The mass flow rate inlet on each nostril will be calculated according to next formula:

$$\dot{m} = Area \text{ nostril} \cdot velocity \text{ inlet} \cdot \rho_{air}$$

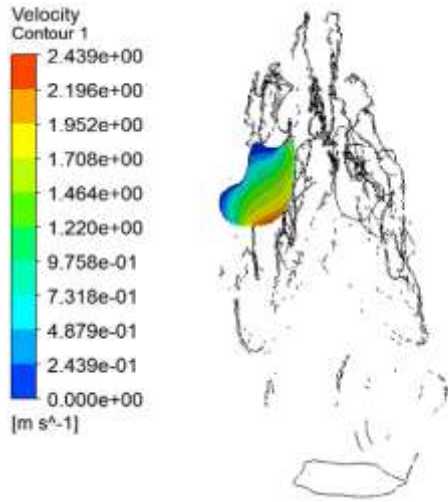


Figure 46. Velocity contour on right nostril model 2

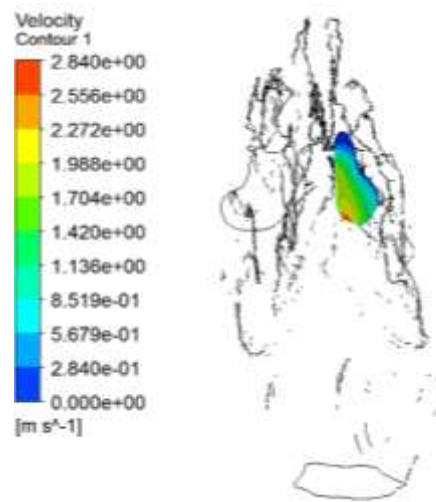


Figure 47. Velocity contour on left nostril model 2

	Area (m ²)	Area Average of velocity (m/s)	Mass Flow Rate (kg/s)
Right Nostril	0,000143846	1,15615	0,0002037
Left Nostril	8,71425 · 10 ⁻⁵	1,19493	0,000127558

Table 17. Air mass flow rate entering on the nostrils in model 2

$$\rho_{air} = \text{air density at } 15 \text{ }^\circ\text{C}, 1.225 \text{ kg/m}^3$$

Comparison of the results with model 1:

	Mass Flow Rate Inlet (kg/s)	
	Right Nostril	Left Nostril
Model 1	0,000153125	0,000153125
Model 2	0,0002037	0,000127558

Table 18. Comparison of model 1 -2 of the air mass flow rate inlet on the nostrils.

Model 3. Sniffing. Extreme conditions breathing.

The convergence of the results is shown in the figure below:

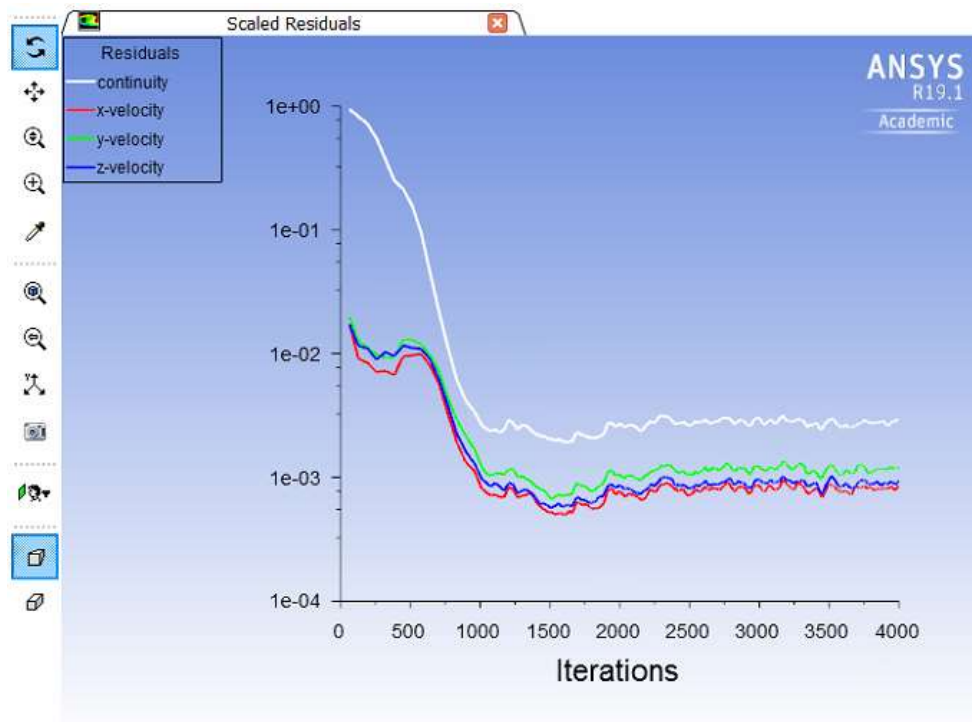


Figure 48. Residuals plot model 3

In this case, the residuals values of the continuity equation are slightly better than when the pressure drop is x5. They reach a value around $2,5 \cdot 10^{-3}$ which can be accepted. The velocity residuals reach values between $1 \cdot 10^{-3}$ and $2 \cdot 10^{-3}$.

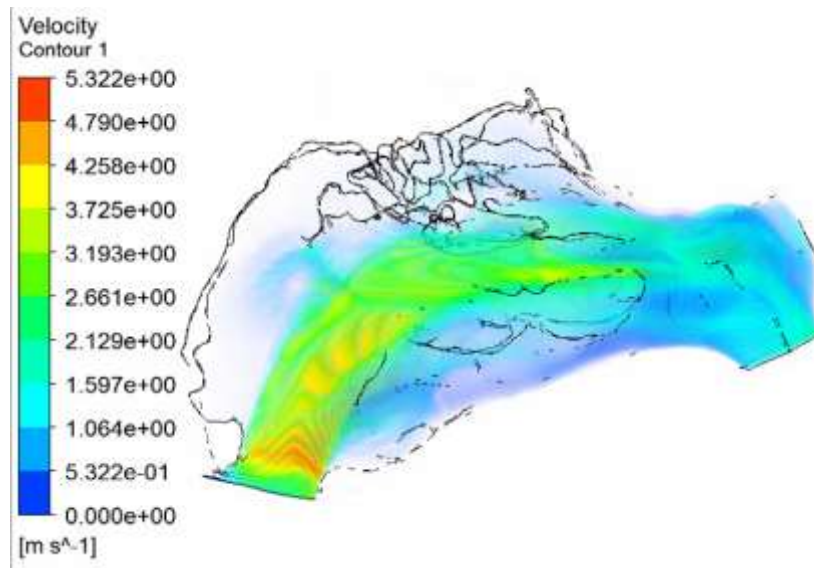


Figure 49. Velocity volume rendering in model 3 view 2

In the figure 58 Velocity volume rendering. It can be checked that the results accomplish the set boundary condition of 0 kg/s of air mass flow rate in the right nostril. As it can see, the air just flows through the left cavity reaching velocities of 5,322 m/s whereas in the case of pressure drop x5 reach 7 m/s. However, the value of the Reynolds number keeps reaching values of a Turbulent flow.

$$Re = \frac{\rho \cdot v_s \cdot D_H}{\mu} = \frac{1,125 \cdot 5,322 \cdot 0,0144}{1,81 \cdot 10^{-5}} \cong 4763 \gg \gg 2100 \quad \text{TURBULENT}$$

$$D_H = \frac{4 \cdot \text{Area}}{\text{Perímetro}} = \frac{4 \cdot 143,85 \cdot 10^{-6}}{0,04} = 0,0144$$

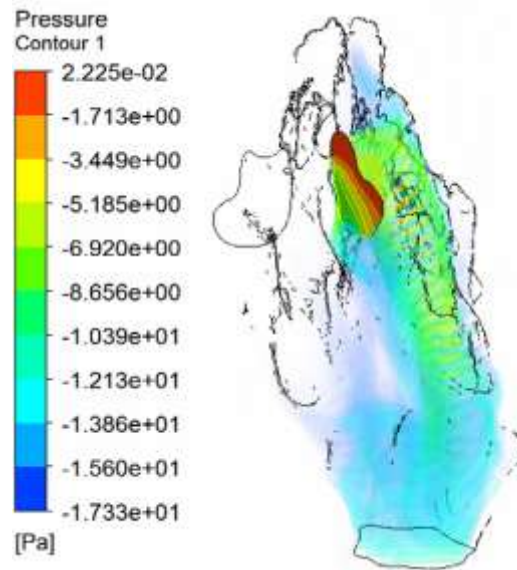


Figure 50. Pressure contour left nostril model 3

The area average pressure on left nostril is -3.84375 Pa.

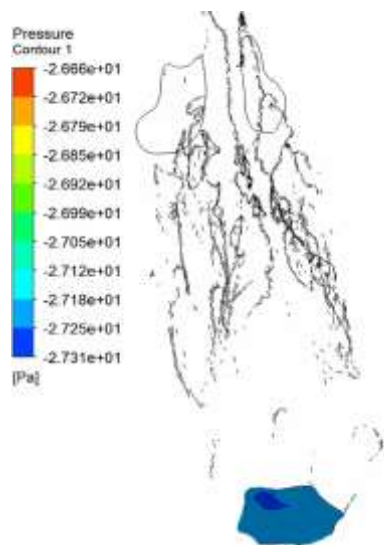


Figure 51. Pressure Outlet Contour in model 3.

The area average of pressure on pressure outlet is -13.6171 Pa.

Then, the pressure drop in model 3 is around:

$$\Delta P = P_{inlet} - P_{outlet} = -3.84375 \text{ Pa} - (-13.6171 \text{ Pa}) = 9,7733 \text{ Pa}$$

This pressure drop is not the same that the set in the model. It implies an error of:

$$\epsilon_{\text{pressure drop}} (\%) = \frac{\Delta P_{set} - \Delta P_{results}}{\Delta P_{set}} = \frac{16,615955 \text{ Pa} - 9,7733 \text{ Pa}}{16,615955 \text{ Pa}} \times 100 = 41,11\%$$

The mass flow rate inlet will be calculated:

$$m = \text{Area left nostril} \cdot \text{velocity inlet} \cdot \rho_{air}$$

$$\text{Area left nostril} = 8,71425 \cdot 10^{-5} \text{ m}^2;$$

$$\text{velocity inlet} = 2,2087 \frac{\text{m}}{\text{s}};$$

$$\rho_{air} = \text{air density at } 15 \text{ }^\circ\text{C}, 1,225 \text{ kg/m}^3;$$

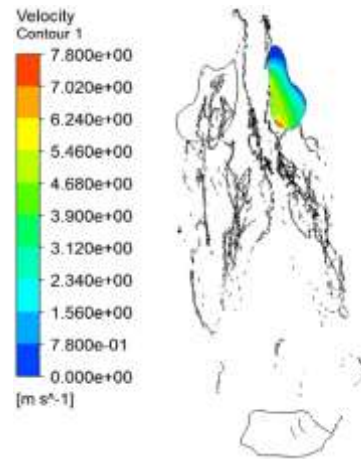


Figure 52. Velocity contour on left nostril model 3

$$\begin{aligned} \dot{m} &= 8,71425 \cdot 10^{-5} \text{ m}^2 \cdot 3,21177 \frac{\text{m}}{\text{s}} \cdot 1,225 \frac{\text{kg}}{\text{m}^3} \\ &= 2,35778 \cdot 10^{-4} \text{ kg/s} \end{aligned}$$

By using the tool streamline is easily to know the number of particles path which reach the Ephemelium Olfactory (EO) Area. In the next figure, it can be appreciated that 4 particles paths reach this area of 100 paths which have been represented:

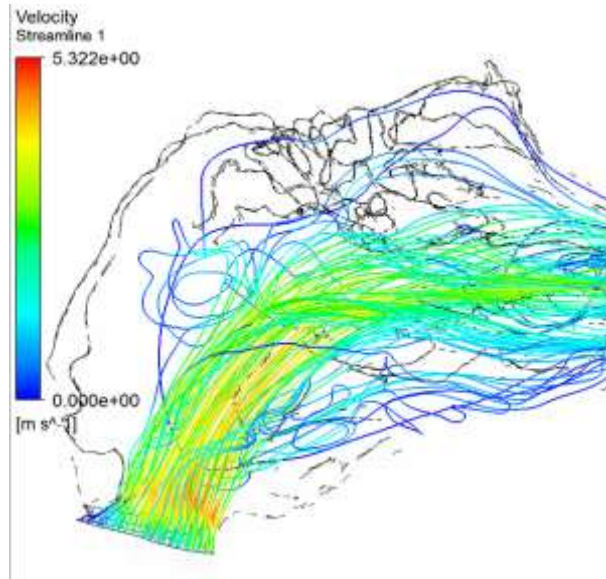


Figure 53. Velocity streamline model 3.

$$\% \text{ particle paths reach EO} = \frac{N^{\circ} \text{ lines reach OE}}{N^{\circ} \text{ lines represented}} = \frac{4}{100} = 4\%$$

Comparison of the results 3 with model 1:

	Mass Flow Rate Inlet (kg/s)	
	Right Nostril	Left Nostril
Model 1. Normal Breathing	0,000153125	0,000153125
Model 3. Sniffing	0	0,000235778
Increment (%)	—	53,98%

Table 19. Comparison of air mass flow rate inlet of model 3 with model 1.

As Table 19 indicates, the mass flow rate inlet in model 3 increases a 53,98% the amount of model 1. That indicates that the results are coherent since the higher the pressure drop the higher the mass flow rate breathed.

Model 4. Particle's injection.

The convergence of the results is represented in the figure below:

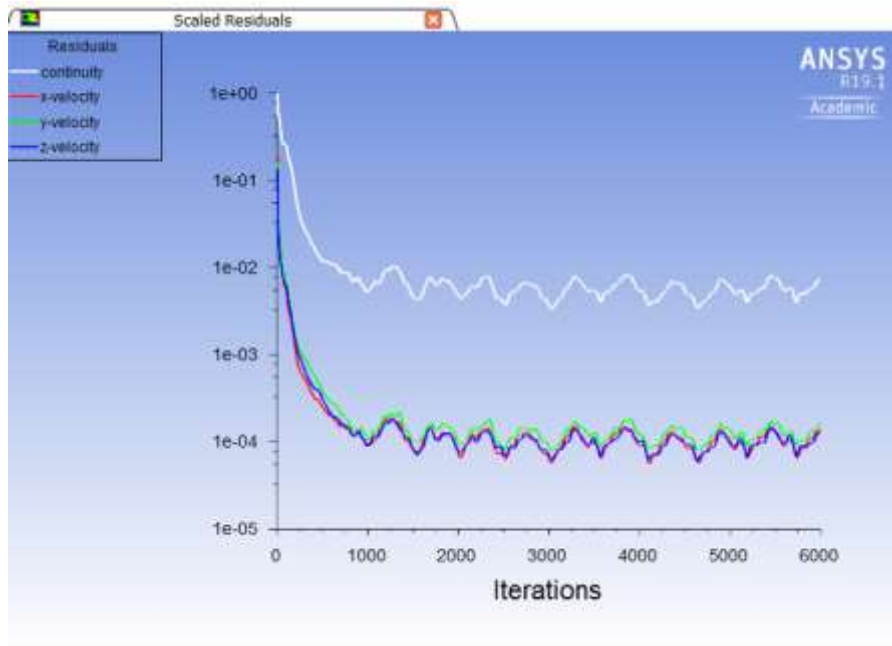


Figure 54. Residuals plot model 4

In this case, the residuals values of the continuity equation are not as good as the previous ones, but they reach a value between $2,5 \cdot 10^{-3}$ and $8 \cdot 10^{-3}$ which can be accepted. The velocity residuals reach values are around $1 \cdot 10^{-4}$.

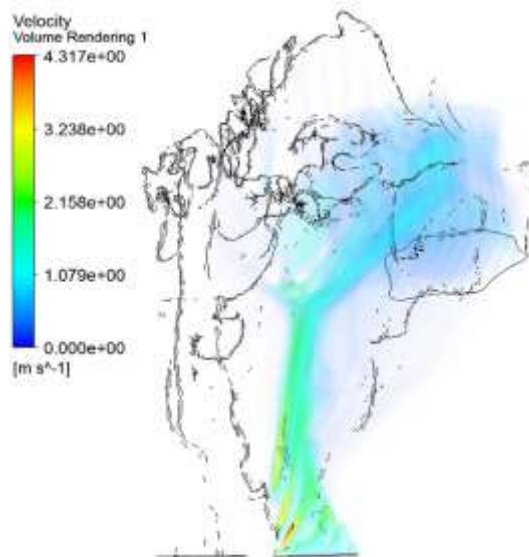


Figure 55. Velocity volume rendering model 4

In the figure 64, Velocity volume Rendering. It can be checked that the results accomplish the set boundary condition of 0 kg/s of air mass flow rate in the right nostril. As it

can see, the air just flows through the left cavity reaching velocities of 4,317 m/s in the entrance of the cavity.

By using the tool streamline, it is easily to know the number of particles path which reach the Epithelium Olfactory (EO) Area. In the next figure, it can be appreciated that 5 particles paths reach this area of 100 paths which have been represented:

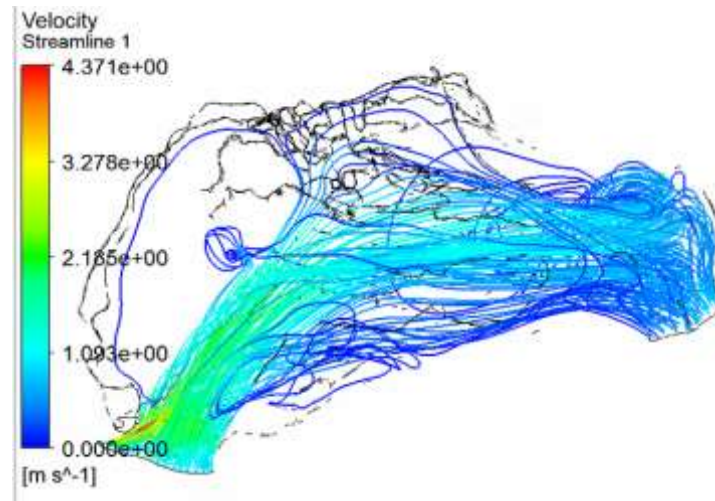


Figure 56. Velocity stream line model 4.

$$\% \text{ particle paths reach EO} = \frac{N^{\circ} \text{ lines reach OE}}{N^{\circ} \text{ lines represented}} = \frac{5}{100} = 5\%$$

8. CONCLUSIONS

The objective of the present thesis is analyse the capacity of the software Ansys Fluent to simulate the human breathing through nasal model file of a patient which has been transferred from an stl.file to AnsysFluent. The main objective has been achieved by the accomplishment of partial objectives:

- First of all, mesh the complex geometry of the nasal cast has been successfully achieved by selecting the patch conforming algorithm and the method tetrahedrons.
- Secondly, a mesh independence study has been carried out letting us choose the finer mesh to obtain higher accuracy in the results.
- Thirdly, after getting a refined mesh different human breathing conditions have been simulated:
 - A normal human breathing capacity by setting up the air mass flow rate inlet. Then, the pressure drop between the nostrils and mouth connection has been calculated.
 - A normal human breathing capacity but by setting up the pressure drop calculated in the first simulation. This second simulation verifies that by setting up different boundary conditions the results are in the same order of magnitude.
 - An extreme conditions of human breathing like sniffing action. A higher pressure drop of two and a half times bigger is set up between inlet and outlet and one cavity is block. This case shows how the bigger the pressure drop the higher the amount of air is breathed.
 - A particles's injection flow is simulated by setting up the average doses of an aerosol in the market.

All the cases have been underwent to post processing analysis. Some of the parameters which have been measured are:

- The reached air flow velocity in some parts of the nose.
- The number of flow particles that reach the OE Olphactive Epitelium Area.

As conclusion, it can be extracted that most of the amount of the flow goes to the connection to the lungs. On the other hand, it is obserbed that the particles trajectory is not influenced neither the pressure drop nor amount of flow injected. Therefore, future research can focus on the simulation of other directions in the simulation of particle's injection or changing the properties of the drug formulation in order to see how affect physicals properties of the drug in the trajectory of the particle (density, particle's size).

REFERENCES

- Alzheimer's Disease International (ADI). (2018). *World Alzheimer Report 2018*. London.
Récupéré sur <https://www.alz.co.uk/research/world-report-2018>
- CE' DRIC GIRERD, I. T. (2018). In Vivo Inspection of the Olfactory Epithelium: Feasibility of Robotized Optical Biops.
- L. Salade, N. W. (2019). How to characterize a nasal product. The state of the art of in-vitro and exvivo specific methods . *International Journal of Pharmaceutics*.
- Mukta Agrawala, S. S. (2018). Nose-to-brain drug delivery: An update on clinical challenges and progress towards approval of anti-Alzheimer drugs. *Journal of Controlled Release*.
- ANSYS Fluent Workbench Tutorial Guide, April 2018
- ANSYS Meshing Advanced Techniques, PADT Lunch & Learn Series
- <https://www.computationalfluidynamics.com.au/convergence-and-mesh-independent-study/>

APPENDICES

ANSYS FLUENT

Due to the computer revolution in the last decades some numerical techniques has been evolved for the solution of equations of fluid dynamics. This revolution has supposed a big step forward because the equations of fluid dynamics are analytically solvable for only a limited number of flows.

CFD has led the birth of a specialised discipline called computational fluid dynamics (CFD)

Tetrahedral Methods

Patch Conforming

- **Bottom up** approach: Meshing process
 - Edges → Faces → volume
- All faces and their **boundaries** are **respected** (conformed to) and meshed (except with defeaturing tolerance)
- Good for high quality (clean) CAD geometries
 - CAD cleanup required for dirty geometry
- Sizing is defined by **global** and/or **local** controls
- Compatible with inflation

To access it

- Insert Method
 - Set to Tetrahedrons
 - Set to **Patch Conforming**

Patch Independent

- **Top down** approach: Meshing process
 - Volume meshed first → projected on to faces & edges
- Faces, edges & vertices **not necessarily conformed**
 - Controlled by tolerance and scoping of Named Selection, load or other object
- Good for gross de-featuring of poor quality (dirty) CAD geometries
- Method Details contain sizing controls
- Compatible with inflation

To access it

- Insert Method
 - Set to Tetrahedrons
 - Set to **Patch Independent**

Details of "Patch Conforming Method" - Method	
Scope	
Scoping Method	Geometry Selection
Geometry	1 Body
Definition	
Suppressed	No
Method	Tetrahedron
Algorithm	Patch Conforming
Element Middle Node	Product of Volume of Faces Patch Independent (P)

1.1. Quality of the mesh

The quality of the mesh plays a significant role in the accuracy and stability of the numerical computation. Regardless of the type of mesh used in your domain, checking the quality of your mesh is essential to obtain a robust simulation. Orthogonality

Minimum cell orthogonality is an important indicator of mesh quality. Values for orthogonality can vary between 0 and 1 with lower values indicating poorer quality cells. In general, the minimum orthogonality should not be below 0.01 with the average value significantly larger. In order to determine the orthogonal quality of a given cell, the following quantities are calculated for each face:

the normalized dot product of the area vector of a face (\vec{A}_i) and a vector from the centroid of the cell to the centroid of that face (\vec{f}_i):

$$\frac{\vec{A}_i \cdot \vec{f}_i}{|\vec{A}_i| |\vec{f}_i|}$$

(equation 1)

the normalized dot product of the area vector of a face (\vec{A}_i) and a vector from the centroid of the cell to the centroid of the adjacent cell that shares that face (\vec{c}_i):

$$\frac{\vec{A}_i \cdot \vec{c}_i}{|\vec{A}_i| |\vec{c}_i|} \quad (\text{equation 2})$$

The minimum value that results from calculating Equation 5–1 and Equation 5–2 for all of the faces is then defined as the orthogonal quality for the cell. Therefore, the worst cells will have an orthogonal quality closer to 0 and the best cells will have an orthogonal quality closer to 1. The Figure 5.22 represents the relevant vectors used to calculate the orthogonal quality and is an example where Equation 5–2 produces the minimum value and therefore determines the orthogonal quality.

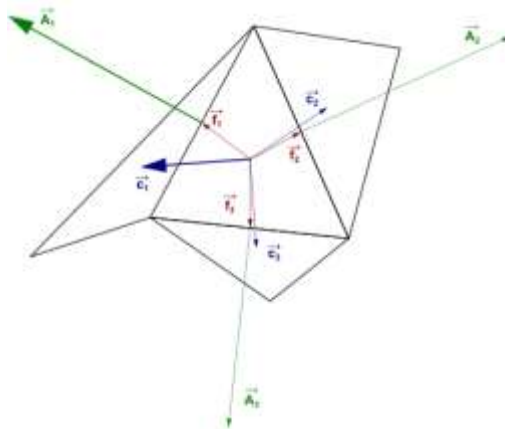


Figure 57. Calculating the cell Orthogonality.

1.1.1. Aspect ratio

Another important indicator of the mesh quality is the aspect ratio. The aspect ratio is a measure of the stretching of a cell. It is computed as the ratio of the maximum value to the minimum value of any of the following distances: the normal distances between the cell centroid and face centroids (computed as a dot product of the distance vector and the face normal), and the distances between the cell centroid and nodes. For a unit cube (see Figure 5.23: Calculating the Aspect Ratio for a Unit Cube), the maximum distance is 0.866, and the minimum distance is 0.5, so the aspect ratio is 1.732. This type of definition can be applied on any type of mesh, including polyhedral.

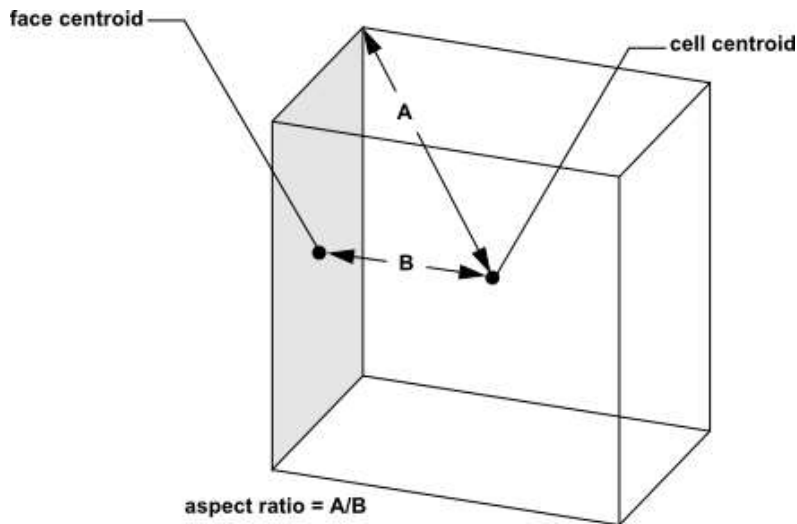


Figure 58. Calculating the aspect ratio

As discussed in Computational Expense, for highly anisotropic flows, extreme aspect ratios may yield accurate results with fewer cells. Generally, it is best to avoid sudden and large changes in cell aspect ratios in areas where the flow field exhibit large changes or strong gradients.

The high aspect ratio cells in this mesh are near the walls and are a result of the boundary layer inflation applied in the meshing step. For more information about the importance of mesh quality refer to the Fluent User's Guide.

To check the quality of your mesh, you can use the Report Quality button in the General task page:



A message will be displayed in the console, such as the example that follows:

```
Mesh Quality:
Orthogonal Quality ranges from 0 to 1, where values close to 0 correspond to low quality.
Minimum Orthogonal Quality = 6.07960e-01
Maximum Aspect Ratio = 5.42664e+00
```

For information about how to improve poor quality cells, see Repairing Meshes.

When evaluating whether the quality of your mesh is sufficient for the problem you are modeling, it is important to consider attributes such as mesh element distribution, cell shape, smoothness, and flow-field dependency. These attributes are described in the sections that follow.

1.1.2. Resolution of the mesh

Resolution of the boundary layer (that is, mesh spacing near walls) also plays a significant role in the accuracy of the computed wall shear stress and heat transfer coefficient. This is particularly true in laminar flows where the mesh adjacent to the wall should obey

Proper resolution of the mesh for turbulent flows is also very important. Due to the strong interaction of the mean flow and turbulence, the numerical results for turbulent flows tend to be more susceptible to mesh element distribution than those for laminar flows. In the near-wall region, different mesh resolutions are required depending on the near-wall model being used. See Model Hierarchy for guidelines.

In general, no flow passage should be represented by fewer than 5 cells. Most cases will require many more cells to adequately resolve the passage. In regions of large gradients, as in shear layers or mixing zones, the mesh should be fine enough to minimize the change in the flow variables from cell to cell. Unfortunately, it is very difficult to determine the locations of important flow features in advance. Moreover, the mesh resolution in most complicated 3D flow fields will be constrained by CPU time and computer resource limitations (that is, memory and disk space). Although accuracy increases with larger meshes, the CPU and memory requirements to compute the solution and postprocess the results also increase. Solution-adaptive mesh refinement can be used to increase and/or decrease mesh density based on the evolving flow field, and therefore provides the potential for more economical use of grid points (and hence reduced time and resource requirements). See Adapting the Mesh for information on solution adaption.

1.1.3. Skewness

Skewness is defined as the difference between the shape of the cell and the shape of an equilateral cell of equivalent volume. Highly skewed cells can decrease accuracy and destabilize the solution. For example, optimal quadrilateral meshes will have vertex angles close to 90 degrees, while triangular meshes should preferably have angles of close to 60 degrees and have all angles less than 90 degrees. A general rule is that the maximum skewness for a triangular/tetrahedral mesh in most flows should be kept below 0.95, with an average value that is significantly lower. A maximum value above 0.95 may lead to convergence difficulties and may require changing the solver controls, such as reducing under-relaxation factors and/or switching to the pressure-based coupled solver.

1.1.4. Smoothness

Truncation error is the difference between the partial derivatives in the governing equations and their discrete approximations. Rapid changes in cell volume between adjacent cells translate into larger truncation errors. ANSYS Fluent provides the capability to improve the smoothness by refining the mesh based on the change in cell volume or the gradient of cell volume. For information on refining the mesh based on change in cell volume, see Gradient Adaption and Volume Adaption.

1.1.5. Flow-Field Dependency

The effect of resolution, smoothness, and cell shape on the accuracy and stability of the solution process is dependent on the flow field being simulated. For example, very skewed cells can be tolerated in benign flow regions, but can be very damaging in regions with strong flow gradients.

Since the locations of strong flow gradients generally cannot be determined a priori, you should strive to achieve a high-quality mesh over the entire flow domain.

1.1.6. Monitoring Residuals

Residuals are the measure of convergence of the iterative approach.

In CFD, after discretization, the partial differential equations are converted in to a set of algebraic equations and each algebraic equation has to be solved for individual control volume (Meshing the whole domain into a number sub domains or control volumes).

Hence, residuals signify the local imbalances of any conserved field variable in individual control volumes.

In an iterative numerical solution, the residual will never be exactly zero. However, the lower the residual value is, the more numerically accurate the solution.

In FLUENT: the scaled residuals for continuity, momentum, energy etc has to be defined in the monitor window, which are generally known as Convergence criteria.

